

Article

Additions to the Taxonomy of the Antarctic Dark-Mouth Skate *Bathyraja arctowskii* (Dollo, 1904), with Descriptions of the Syntypes and Morphology of Teeth, Dermal Denticles and Thorns

Simon Weigmann ^{1,*} and Thomas Reinecke ²¹ Elasmolab, Elasmobranch Research Laboratory, Sophie-Rahel-Jansen-Str. 83, 22609 Hamburg, Germany² Independent Researcher, Auf dem Aspei 33, 44801 Bochum, Germany; treinecke@web.de

* Correspondence: simon.weigmann@elasmolab.de

Abstract: The taxonomy of the enigmatic dark-mouth skate, *Bathyraja arctowskii* (Dollo, 1904), from the Southern Ocean was finally resolved after more than 100 years of ambiguity in 2021. This species is the smallest known species of the species-rich deep-water skate genus *Bathyraja* Ishiyama, 1958, which attains a total length of only about 61 cm and appears to be a wide-ranging and locally common species in the Southern Ocean. It differs from its congeners in the small adult size, dark-pigmented mouth cavity and underside of nasal curtain, lack of thorns on upper disc, as well as small and slender egg cases. Although the identity of this species was unambiguously clarified, the syntype egg cases could not be examined due to the COVID-19 pandemic. This examination has now become possible, and detailed data of the syntypes are provided in the present paper for the first time, together with hitherto unknown details of tooth, dermal denticle and thorn morphology. Furthermore, a lectotype and two paralectotypes are designated from the syntypes.

Keywords: odontology; ichthyodorulites; microscopic morphology; egg capsules; Southern Ocean; Arhynchobatidae; Rajiformes; Elasmobranchii; Chondrichthyes



Citation: Weigmann, S.; Reinecke, T. Additions to the Taxonomy of the Antarctic Dark-Mouth Skate *Bathyraja arctowskii* (Dollo, 1904), with Descriptions of the Syntypes and Morphology of Teeth, Dermal Denticles and Thorns. *Diversity* **2023**, *15*, 899. <https://doi.org/10.3390/d15080899>

Academic Editor: Michael Wink

Received: 25 June 2023

Revised: 26 July 2023

Accepted: 26 July 2023

Published: 30 July 2023



Copyright: © 2023 by the authors. Licensee MDPI, Basel, Switzerland. This article is an open access article distributed under the terms and conditions of the Creative Commons Attribution (CC BY) license (<https://creativecommons.org/licenses/by/4.0/>).

1. Introduction

The skates are currently considered to contain about 304 species in two highly diverse (the Arhynchobatidae, or softnose skates, and the Rajidae, or hardnose skates) and two small (the Anacanthobatidae, or legskates, and the Gurgesiellidae, or pygmy skates) families [1–4]. The Arhynchobatidae comprise 13 genera with about 109 species, reaching maximum sizes of 28–203 cm in total length (TL) and occurring in 0–3280 m of depth in all oceans, with the center of distribution in polar and cool temperate regions. The family Rajidae comprises 16 genera with about 160 species, attaining maximum sizes of 33–264 cm TL and occurring at 0–4156 m depth in all oceans, with the center of distribution in cold water on continental slopes and abyssal plains. The Anacanthobatidae include five genera with 16 species, reach maximum sizes of 29–75 cm TL and occur in 150–1725 m of depth on continental and insular slopes of the Central-West Atlantic Ocean, Southwest Indian Ocean and Indo-West Pacific Ocean. The Gurgesiellidae contain 3 genera with 19 species, attain 23–59 cm TL and occur in 39–1096 m of depth in warm temperate and tropical seas of the Atlantic, Indian and Pacific Oceans. All data in this paragraph were updated from [5,6] while considering [1–4]. The genus *Bathyraja* Ishiyama, 1958 is by far the most speciose genus of softnose skates, containing 52 valid species [7]. Additionally, the four valid species currently assigned to *Rhinoraja* Ishiyama, 1952 likely belong to the same genus due to a lack of pronounced morphological and molecular differences [5,7], with species of *Rhinoraja* being deeply nested within the genus *Bathyraja* [7].

An overview of the characteristics and distributions of softnose skates in general has been provided by Last et al. [2], and for the Southern Ocean by Weigmann et al. [8]. Currently, six described and one undescribed species belonging to the genus *Bathyraja* are

considered to occur in the Southern Ocean, representing the only softnose skate genus occurring in this area. The species of *Bathyraja* can be found throughout Antarctic continental waters and around sub-Antarctic islands, where they are the dominant rajiform group [8]. However, the center of distribution of the two closely related deep-water genera *Bathyraja* and *Rhinoraja* together lies in the northwestern Pacific, where almost half of the species occur [5]. In general, three morphotypes of shallow-water, transitional and deep-water species have been characterized [9], the latter so far not having been reported from the Southern Ocean [8]. The three morphotypes differ in size, squamation, color pattern and depth range [9]. In the Southern Ocean, species of *Bathyraja* range from small (to about 60 cm TL) to rather large (to about 160 cm TL) in size and have been reported from the Ross Sea, around Kerguelen and Heard islands, from the continental margin in the Indian Ocean sector, the Weddell Sea, the Lazarev Sea, around the Antarctic Peninsula, South Shetland and South Orkney islands, and at the deep slope of South Georgia [8].

Bathyraja arctowskii is the smallest known species of the genus, reaching only about 61 cm total length (TL) and maturing at around 36–50 cm TL [7]. It is a species of transitional morphotype [9] that can be further differentiated from its congeners by the, at least partial, dark pigmentation of its mouth cavity and underside of its nasal curtain, which are light in other species [7]. *B. arctowskii* is also an exceptional case in skate taxonomy, as it was named by Dollo in 1904 based only on three empty egg cases of tiny size from off the Antarctic Peninsula [10]. As such, the species remained undescribed for more than 100 years. The reason was the lack of specimens that could be assigned to Dollo's small egg cases. While examining a large collection of 276 skates and 40 egg cases from Antarctic waters stored in the Zoological Museum Hamburg, Germany (ZMH), SW found an egg case that contained a near-term embryo. A comparison of the embryo with other specimens of different maturity stages and sexes proves their conspecificity [7]. Previously, *B. arctowskii* had been treated as a *nomen dubium*, and skates belonging to this species were confused with the much larger *B. griseocauda* (Norman, 1937) by Bigelow & Schroeder [11] and Springer [12]. Although finally the identity of *B. arctowskii* was unambiguously clarified by Stehmann et al. [7], the syntype egg cases could not be examined at that time due to the COVID-19 pandemic. This has now become possible, and detailed data of the syntypes are provided in the present paper for the first time, together with hitherto unknown details of the tooth, dermal denticle and thorn morphology. Furthermore, a lectotype and two paralectotypes are designated from the syntypes. The detailed comparison of the type egg cases with the egg cases stored in the ZMH (including the aforementioned egg case with a near-term embryo) provides further evidence of their conspecificity.

2. Materials and Methods

One adult male (ZMH 115243, 502 mm TL) and one adult female (ZMH 115243, 510 mm TL) were sampled for teeth by cutting a strip of tissue (with several teeth) from the symphyseal, lateral and commissural regions of the upper (palatoquadrate) and lower jaw (mandible). To obtain individual, clean teeth for photographic documentation, the tissue enclosing the roots was weakened and partly destroyed in a strongly alkalic solution prepared by dissolving 2–3 solid KOH pastilles in ca. 3 mL water (for each strip) in a small glass or PE vessel. The process of weakening the cohesion and releasing the teeth from the tissue was monitored under binoculars and took 45–120 min. Any adhering organic material was removed under the microscope using tweezers and a thin needle. After rinsing in water, the teeth were cleaned in an ultrasonic bath for 10–15 s.

Samples of the squamation were cut from five positions on the dorsal sides, which were equivalent in the female and male individuals but with one additional alar thorn sample in the male. The schematic drawing in Figure 1 illustrates the terminology and position of the different pattern components of thorns/thornlets and denticles composing the squamation. The process for separating the denticles/thornlets/thorns from the skin was the same as described above for the teeth, but special care had to be taken to avoid damaging the delicate basal root extensions of the denticles.

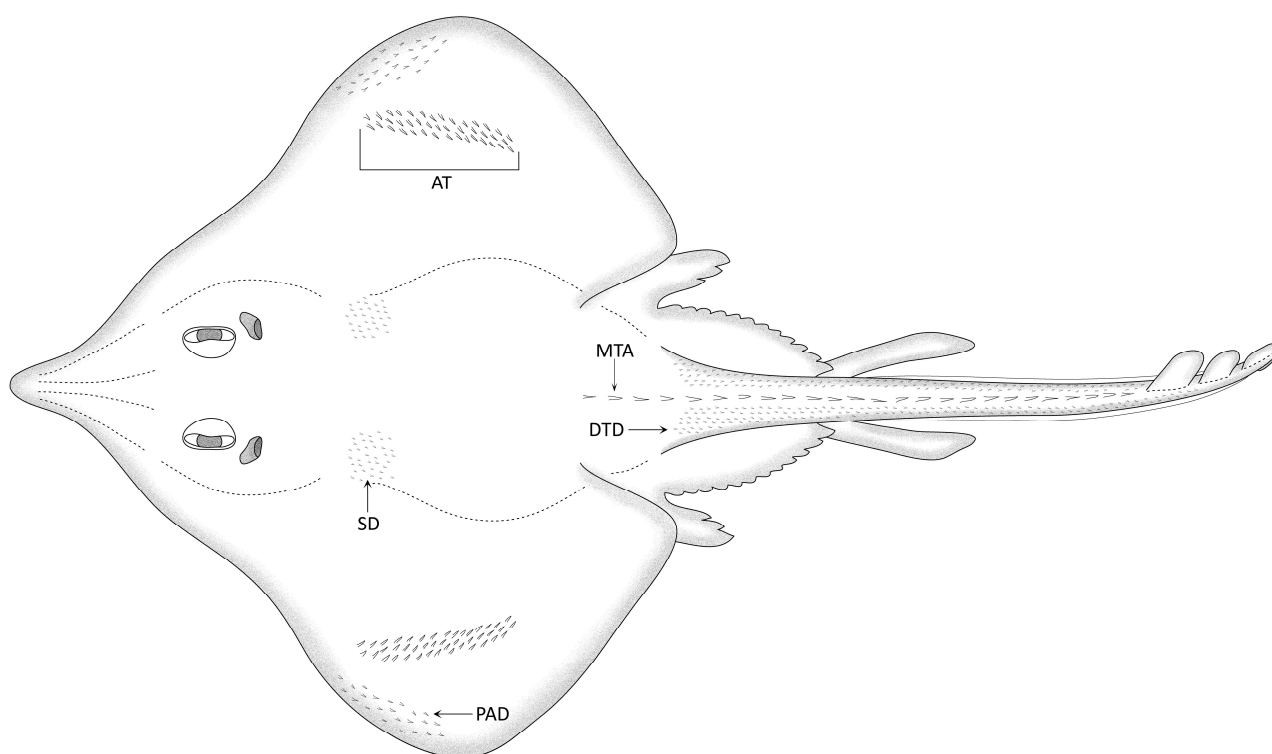


Figure 1. Drawing of a hypothetical rajoid skate in total dorsal view, showing terminology of thorn and dermal denticle pattern components. Thorns and denticles are only depicted in areas where samples were taken; those in other areas are not drafted. The size, number, extent and morphology of thorns and denticles does not reflect the real conditions but schematically indicates the locations where samples were taken. Abbreviations: AT = alar thorns; DTD = dorsolateral tail denticles; MTA = median tail thorns; PAD = pectoral-fin apex denticles; SD = scapular denticles.

The dry teeth and denticles/thorns were fixed with colorless fast-drying nail varnish on the tips of metal or glass fixing pins, previously glued in small brass tubes for easier manipulation under the microscope. If the fixation point is chosen correctly, usually the outermost tip of a root lobe, four to five standard directions (occlusal, basal, labial, lingual and profile views) can be photographed in a single pass. Before imaging, the teeth were stained in a solution of red nail varnish in acetone (1:6 to 1:10 ratios), kept in a small glass vessel and protected against evaporation by a ground-in glass lid. This treatment improves the spatial depth and contrast of the images, in particular for smooth or poorly textured crown surfaces occurring in many teeth. The teeth and denticles/thorns were photographed with a Keyence VHX-950F digital microscope, equipped with a VHX-6020 camera, VH-Z20T zoom objective (20–200× magnification) and a strong diffusor.

Descriptions of the methodology used for taking external and skeletal morphometric measurements, meristics and egg case measurements can be found in the study by Stehmann et al. [7]. The morphological description of the egg cases follows [7,13–17]. The maturity stages are according to [18,19]. The terminology of rajoid tooth morphology follows Ward [20] (text-fig. 1), with additions by Herman et al. [21] (text-fig. 1). In contrast to Herman et al. [21] and in agreement with Ward [20], we prefer the terms “labial” and “lingual” instead of “external” and “internal”, respectively (in conjunction with crown/root surface, view, etc.). Definitions of heterodonty are derived from Cappetta [22] (p. 13). The terminology of denticle morphology follows Gravendeel et al. [23], while the terminology of thorn morphology follows Bustamante et al. [24]. The superordinate term “dermal denticles” is used in our study for all morphological types, independent of their size. Differentiation between denticles, thornlets, and thorns is based on their size, following Bustamante et al. [24]: denticles are less than about 2 mm in height (in subadults and

adults), whereas thornlets are similar in shape but larger and more robust than denticles and usually more than 3 mm high (subadults and adults). Thorns are doubling thornlets in size and height (usually 6–8 mm in height in subadults and adults). Bustamante et al. [24] reported the size of thorns erroneously as 60–80 mm. Although the median tail thorns of *Bathyrāja arctowskii* are smaller than the tail thorns of many other *Bathyrāja* spp., they are still called thorns rather than thornlets due to their equivalence. Institutional acronyms follow Sabaj [25].

Nomenclatural Acts: the electronic edition of this article conforms to the requirements of the amended International Code of Zoological Nomenclature. Hence, the new names contained herein are available under that Code from the electronic edition of this article. This published work and the nomenclatural acts it contains have been registered in ZooBank, the online registration system for the ICZN. The ZooBank LSIDs (Life Science Identifiers) can be resolved, and the associated information viewed through any standard web browser by appending the LSID to the prefix “<https://zoobank.org/>”. The LSID for this publication is urn:lsid:zoobank.org:pub:90806841-080A-4F73-B810-8960BCFDF526. The electronic edition of this work was published in a journal with an ISSN and was archived. It is now available from the following digital repositories: CLOCKSS, Swiss National Library (Helveticat).

3. Results

Systematic account

Family Arhynchobatidae Fowler, 1934

Genus *Bathyrāja* Ishiyama, 1958

Bathyrāja arctowskii (Dollo, 1904)

English vernacular name: Antarctic dark-mouth skate

Figures 2–7; Table 1

Raja arctowskii Dollo, 1904—Poissons in: Expédition Antarctique Belge 1897–99 Zoologie, Antwerpen 1904: 11, 51, 52, plate IX, fig. 10. Types: three empty egg cases IRSNB 25 [orig. 3005], IRSNB 26 [orig. 3006], IRSNB 27 [orig. 3007]; Norman [26]: 5; Weigmann [5]: 953; Last et al. [27]: 17.

Bathyrāja arctowskii (Dollo, 1904)—Stehmann et al. [7]: 1–27; Franzese et al. [28]: 92, 99, 105.

Bathyrāja griseocauda (not Norman, 1937)—Springer [12]: 5–7, figs. 2 and 4b; Iwami & Abe [29]: 58, 60, 61.

Bathyrāja n. sp. (dwarf)—Hanchet et al. [30]: 621, 631.

Bathyrāja sp. 2—Stehmann [31]: 209; Stehmann [9]: 263; Jones et al. [32]: 53, 54, 63 [erroneously as *Bathyrdraco* sp. 2], 64; Kalisz [33]: 4–24.

Bathyrāja sp.—Stehmann & Bürkel [34]: 88, 94.

Bathyrāja sp. (dwarf)—Smith et al. [35]: 1170–73, 1175–78.

Breviraja griseocauda (not Norman, 1937)—Bigelow & Schroeder [11]: R43–R46, fig. 4.

We herein designate syntype **IRSNB 25** [orig. 3005], housed in the collection of the Institut royal des Sciences naturelles de Belgique, as the lectotype of *Bathyrāja arctowskii* (Dollo, 1904) and the two other syntypes, **IRSNB 26** [orig. 3006] and **IRSNB 27** [orig. 3007], as the paralectotypes of *B. arctowskii* (Dollo, 1904).

For a full list of material examined, see Stehmann et al. [7]. The following material is depicted in the Figures 2–7 of the present study (4 egg cases, 6 skate specimens):

Lectotype **IRSNB 25** [orig. 3005], 71°19′ S, 87°37′ W, 27–28 May 1898, 435 m depth; paralectotype **IRSNB 26** [orig. 3006], 70°23′ S, 82°47′ W, 7–8 October 1898, 400 m depth; paralectotype **IRSNB 27** [orig. 3007], 70°15′ S, 84°06′ W, 19–20 December 1898, 569 m depth; **ZMH 9014**, one empty egg case, 77.6 mm egg case length (ECL), one near-term male embryo, 120 mm TL (removed from egg case, 76.1 mm ECL, also catalogued under ZMH 9014), 61°13.9′ S, 56°25.4′ W, 21.11.96, 403–415 m depth; **ZMH 115243** (ex ISH 689-1978), one adult male, 502 mm TL, and one adult female, 510 mm TL, taken together with two juvenile males, 299 and 346 mm TL, one adult males, 520 mm TL, two adult females, 492 and 535 mm TL (all damaged), 60°53′ S, 55°19′ W, 24.01.78, 345–400 m depth; **ZMH 121822** (ex ISH 37-1984), one juvenile female, 236 mm TL, and one subadult male, 424 mm TL,

taken together with 92 specimens, males 141–432 mm TL, females 135–475 mm TL, 61°11' S, 56°12' W, 13.11.83, 375 m depth; **ZMH 120216** (ex ISH 489-1981), one adult male, 533 mm TL, taken together with one female, 347 mm TL, one juvenile male, 327 mm TL, 60°51' S, 55°34' W, 18.03.81, 280–294 m depth.

Stehmann et al. [7] already provided a detailed diagnosis and description of *B. arctowskii*. An updated diagnosis and description of *B. arctowskii* is provided in the present paper, based on the same specimens but considering new information on the lectotype and paralectotype egg cases and the morphology of teeth, dermal denticles and thorns.

3.1. Diagnosis (Updated from Stehmann et al. [7])

Bathyraja arctowskii is the smallest known species of the species-rich genus *Bathyraja*, attaining only about 61 cm TL based on more than 300 specimens examined. It is characterized by an evenly inverse heart-shaped disc (with distinctly undulated margins in adult males) with broadly rounded outer corners and with body length to mid-cloaca shorter than or equal to tail length from mid-cloaca. Preorbital snout length 8.1–16.2% TL, depending on ontogenetic stage, and distance between first gill slits 14.2–15.9% of TL. Orbits moderately large, horizontal diameter 1.3–1.8 times interorbital width. Jaws weakly angled, with 22–29 upper and 21–29 lower tooth rows, arranged in parallel rows in adult males but in quincunx pavement pattern in females and juvenile males. Sexual dimorphism also apparent in individual teeth, which have a pronounced triangular cusp in adult males but a low cusp in females and juvenile males. Upper side of disc and tail entirely rough prickly with dermal denticles, underside smooth. Individual denticles of star or cross type and mostly with a pronounced, hook-like cusp. Except for non-retractable, hook-like alar thorns of mature males, no thorns on disc but only a median row of 19–30 small thorns along tail to first dorsal fin. The blunt-tipped, circular-based tail thorns become smaller and more widely spaced posteriorly in subadults and adults and are generally wider-spaced in large juveniles to adults as compared to small juveniles. Bases of low, more or less equal-sized dorsal fins confluent or with short interspace. Postdorsal tail section very short, 1.7–5.2% TL, with low epichordal caudal lobe which is confluent with second dorsal fin. Dorsal ground color plain dark to medium grayish-brown, often with mostly indistinct scattered pale and dusky spots on disc, posterior pelvic lobes and on sides of tail, occasionally with transverse pseudocellus-stripe on inner posterior pectorals. Underside mostly plain white or pale, often with gray marked cloaca and gray spots on belly to gill region, occasionally gray spotted posterior pectoral margins, origin and sides of tail, or tail partly dark. Mouth cavity and underside of nasal curtain at least partly, usually completely pigmented medium to dark grayish from very small juvenile stages onwards. Opened clasper tip shows all components typical for *Bathyraja* species, of which most apparent a long and deep pseudosiphon (ps) along outer edge of dorsal lobe, as well as a massive projection (pj) over entire length of the inner ventral lobe. Clasper terminal skeleton with distal processes of dorsal marginal cartilage (forming external pseudorhipidion) and ventral marginal cartilage (forming external projection), three dorsal terminal cartilages (with dt1 very large and encapsulating terminal skeleton), ventral terminal and one accessory terminal cartilage. Sexual dimorphism apparent in scapulocoracoid, with post-mesocondyle length longer in females than in males. Both surfaces of blackish-brown egg cases smooth, with coverage of long, fine anchoring fibers. Extension of aprons two-thirds onto horns. Upper side of egg cases strongly convex, lower side moderately convex. Cross-section (anterior and posterior horns) depressed. *B. arctowskii* differs from its congeners in the small adult size, dark-pigmented mouth cavity and underside of nasal curtain, lack of thorns on upper disc, as well as small and slender egg cases.

3.2. Description

Based on Stehmann et al. [7], a condensed and updated description of the external and skeletal morphology of *B. arctowskii* is provided in the present paper, based on the same specimens as in Stehmann et al. [7], but considering new information on the morphology

of teeth, dermal denticles and thorns. For more details on other descriptive aspects, the reader is referred to the description section in Stehmann et al. [7]. In addition, detailed descriptions of the lectotype and paralectotype egg cases, as well as ontogenetic changes and sexual dimorphism are given.

3.2.1. External Morphology

Disc evenly inverse heart-shaped, anterior margins not to strongly undulated, outer corners of disc broadly rounded. Disc width 1.2–1.4 times disc length, markedly wide. Axis of maximum disc width at 24.2–31.9% TL, or 54.1–61.0% of disc length, and distinctly posterior to shoulder girdle. Dorsal head length 14.2–21.6% TL. Snout tip somewhat pronounced, narrowly rounded; snout moderately elongated and pointed at 110–140°, with preorbital length 8.1–16.2% TL and 2.2–5.3 times the narrow interorbital width. Orbit horizontal diameter 1.3–1.8 times interorbital width and 1.5–2.0 times length of spiracle depression; interspiracular space wide, 2.2–2.6 times interorbital space; about 10 pseudobranchial folds in each spiracle. Tail slender, gradually tapering towards tip; a low triangle in cross-section, width at level of pelvic tips 1.1–1.8 times height, width at first dorsal-fin origin 1.1–2.6 times height; tail length from mid-cloaca 1.0–1.5 times distance snout tip to mid-cloaca. Both dorsal fins parallelogram-shaped with broadly rounded upper margin and somewhat frayed tip widely overhanging base end; posterior margin strongly inclined forward and concave; both dorsal fins about as long as high, base of first dorsal fin 0.6–1.6 times that of second dorsal fin. Bases of both dorsal fins confluent or with very small interspace. Postdorsal tail short, 47.4–155.6% of second dorsal-fin base length, with a low and indistinct epichordal caudal fold confluent with second dorsal fin, height of epichordal lobe 0 to ~30% of second dorsal-fin height; hypochordal caudal fold absent. Lateral tail folds along posterior two thirds to full tail length.

Ventral head length 25.0–28.0% TL. Preoral snout length 1.5–2.3 times internarial width and 1.2–2.4 times mouth width, the latter 22.9–36.7% of ventral head length and 97.5–129.4% of internarial space; ventral head length 3.2–4.3 times internarial space; distance between fifth gill slits 58.5–81.9% of distance between first gill slits, the latter 2.1–2.4 times internarial space. Anterior nasal flaps rather small and smooth-edged. Outer edges of nasal curtain smooth and not notched, apices rounded, their outer margin smooth; rear margin of curtain weakly fringed by broad and fleshy fringes; isthmus deeply arc-shaped. Anterior and posterior pelvic-fin lobes separated by a deep notch, posterior lobe with angular outer margin and rounded tip 1.1–1.6 times longer than solid anterior lobe tapering to a blunt tip. Fully developed claspers long and slender, with terminal region only somewhat widened; distal half of clasper stem plus terminal region exceeding tips of posterior pelvic lobes; clasper postcloaca length about half of tail length from mid-cloaca.

Jaws weakly angled, with 22–29 upper and 21–29 lower tooth rows. As typical for the genus (and many other rajoid genera), dentitions of *B. arctowskii* show gradient monognathic heterodonty and lack dignathic heterodonty. Sexual heterodonty is apparent by the presence of a well-developed crown with more or less triangular, pointed cusp in teeth of adult males, whereas teeth of adult females have a rather low crown with lingually displaced cusp. Furthermore, the teeth are arranged in parallel rows in adult males but in quincunx pavement pattern in females and juvenile males. Only teeth of males present ontogenetic heterodonty, bearing a low crown with small cone missing cutting edges in juveniles that grows to a distinct cusp with maturing.

Individual teeth of adult males (Figure 2) with suboval crown base, being almost as wide as long (in occlusal view), and curved basally at labial and lingual crown margins (in lingual and profile view). Labial visor rather thin (in profile view), with a weak to absent apron. Uvula (= medial lingual crown base) slightly angular and warped in basal direction. Crown of symphyseal/anterior teeth moderately high with symmetrical to oblique cusp, strongly inclined lingually and thereby projecting the lingual crown base (in profile/basal view). Transverse cutting edge of the cusp extending continuously from near the crown base to the crown apex. Labial cutting edge absent. Labial and lingual

crown surfaces smooth. Labial surface mesio-distally rather flat, but apico-basally curved in symphyseal to anterior teeth and changing to almost straight in lateral to commissural teeth. Holaulacorhizid root slightly lower (in symphyseal/anterior teeth) or higher than crown (in lateral/commissural teeth). Root stem well developed, oval shaped in cross-section, strongly widening in basal direction and giving way to two, often differently thick root lobes that are separated by a deep median groove with a single large foramen. Basal root surfaces flat to slightly concave.

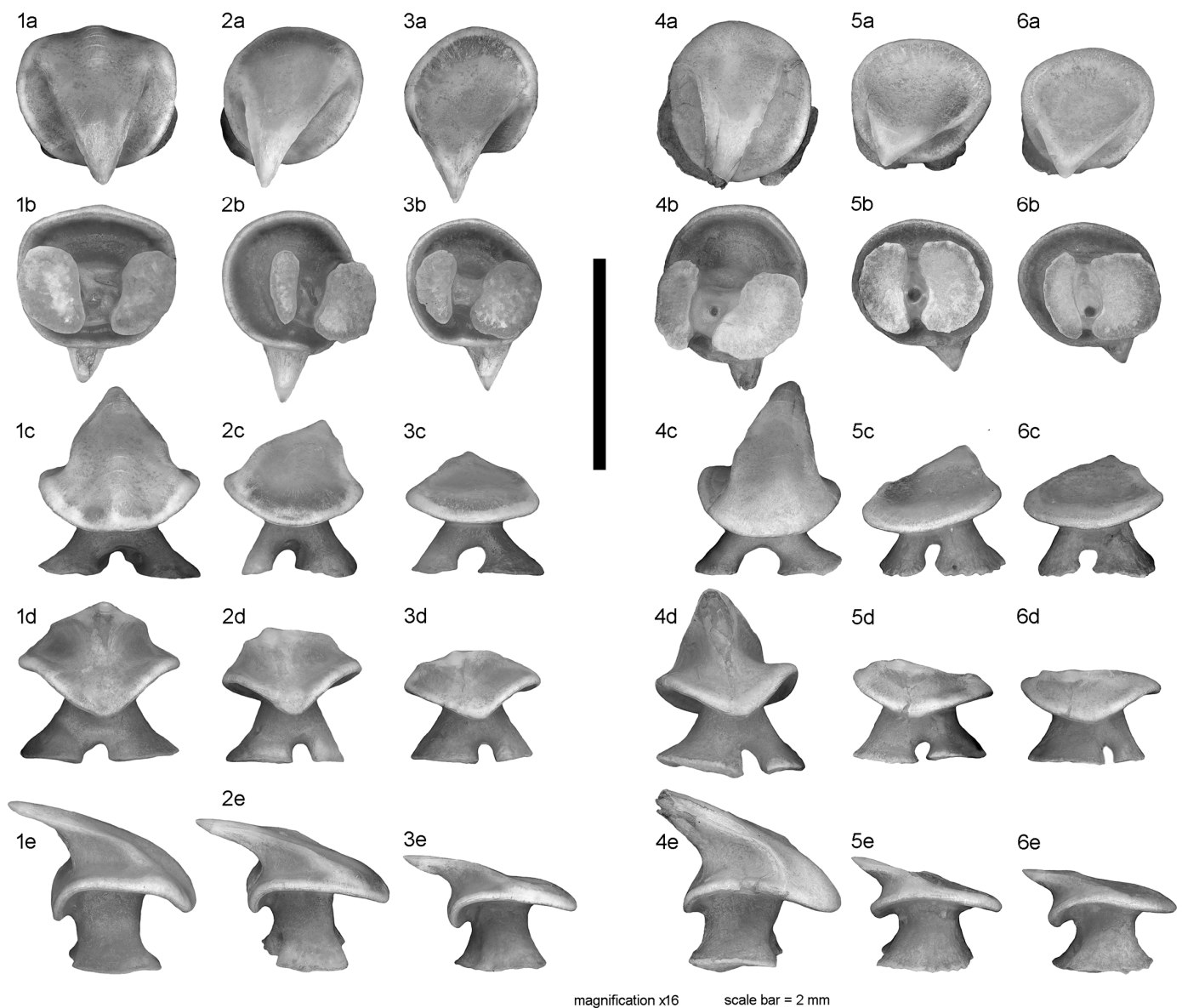


Figure 2. *Bathyraja arctowskii*, ZMH 115243, adult male, 502 mm TL. (1–3) selected teeth of lower jaw; (1a–e) symphyseal region, H = 1.71 mm, W = 1.53 mm, L = 1.37 mm; (2a–e) lateral region, H = 1.41 mm, W = 1.34 mm, L = 1.36 mm; (3a–e) lateroposterior region, H = 1.13 mm, W = 1.27 mm, L = 1.23 mm. (4–6). selected teeth of upper jaw; (4a–e) symphyseal region, H = 1.65+ mm, W = 1.35 mm, L = 1.50 mm; (5a–e) lateral region, H = 1.07 mm, W = 1.32 mm, L = 1.24 mm; (6a–e) lateroposterior region, H = 0.99 mm, W = 1.29 mm, L = 1.20 mm. (1a–6a) = occlusal views; (1b–6b) = basal views; (1c–6c) = labial views; (1d–6d) = lingual views; (1e–6e) = profile views.

Teeth of adult females (Figure 3) with sub-circular to oval crown base, nearly as wide as long to wider than long in posterior/commissural teeth (in occlusal view). Crown lower or much lower than root (in profile view). Cusp pointed but low, strongly displaced

lingually (in occlusal/profile view), and commonly slightly oblique in distal direction (except in symphyseal/anterior-most teeth). Cusp in profile view lingually directed except in posterior/commissural teeth which have an upright cusp. Uvula, apron and ornamentation absent. Lingual face in profile view concave, labial one flat to slightly convex. Root characteristics very similar to those of male teeth.

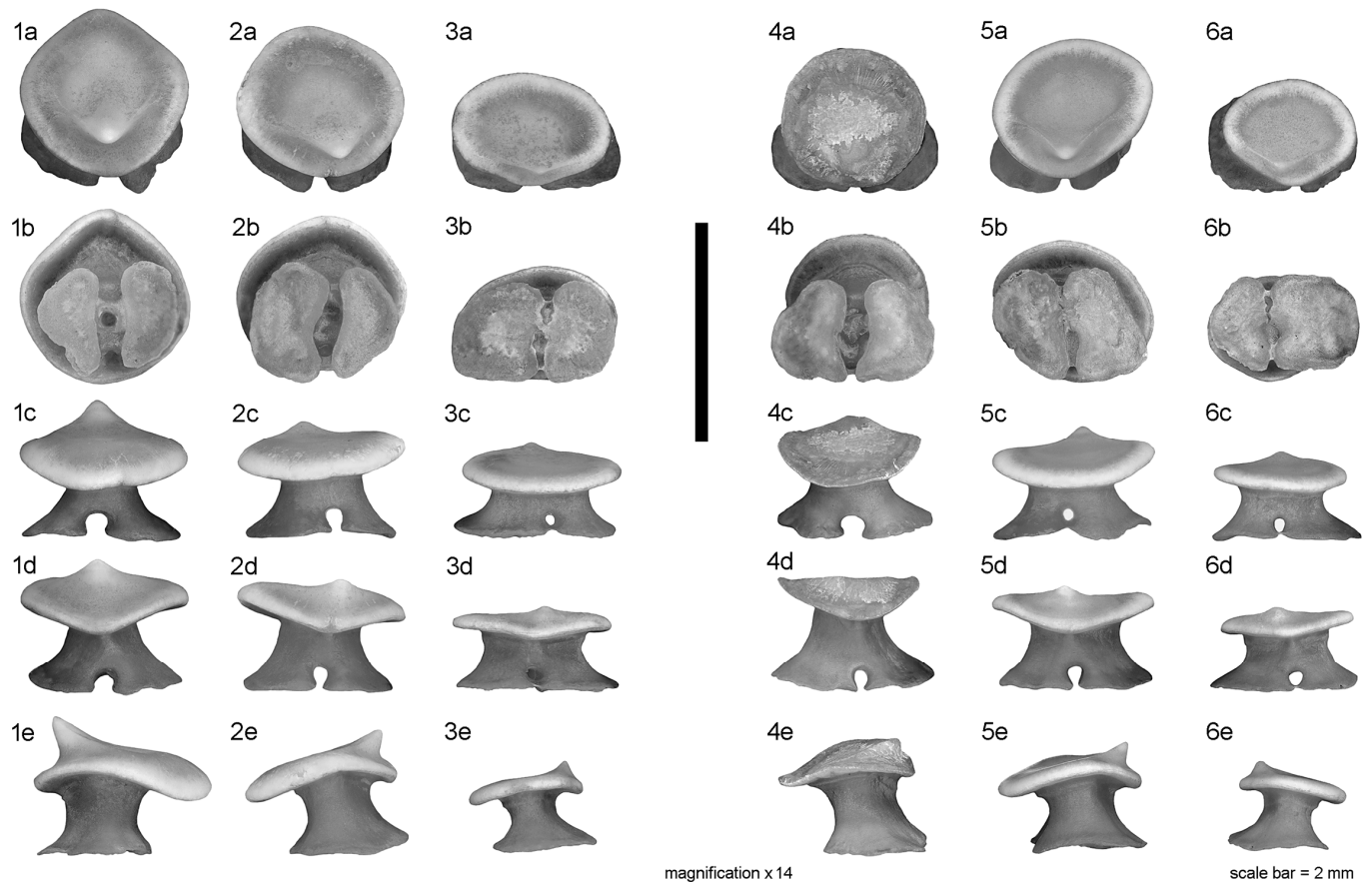


Figure 3. *Bathyraja arctowskii*, ZMH 115243, adult female, 510 mm TL. (1–3) selected teeth of lower jaw; (1a–e) symphyseal region, H = 1.24 mm, W = 1.55 mm, L = 1.62 mm; (2a–e) lateral region, H = 1.15 mm, W = 1.54 mm, L = 1.39 mm; (3a–e) lateroposterior region, H = 0.78 mm, W = 1.45 mm, L = 1.03 mm. (4–6) selected teeth of upper jaw; (4a–e) symphyseal region, H = 1.06+ mm, W = 1.33 mm, L = 1.27 mm; (5a–e) lateral region, H = 0.97 mm, W = 1.49 mm, L = 1.31 mm; (6a–e) lateroposterior region, H = 0.82 mm, W = 1.22 mm, L = 0.99 mm. (1a–6a) = occlusal views; (1b–6b) = basal views; (1c–6c) = labial views; (1d–6d) = lingual views; (1e–6e) = profile views.

No thorns on upper disc except for very elongated field of alar thorns across outer pectoral corners and parallel to anterior half of posterior margins; alar thorns hook-like and of non-retractable, permanently erect type; alar thorns set in three to five longitudinal and about 20 transverse rows. Tail with 19–30 median thorns from between pelvic and pectoral insertions to somewhat anterior to first dorsal-fin base. The tail thorns become smaller and more widely spaced posteriorly in subadults and adults and are generally wider-spaced in large juveniles to adults as compared to small juveniles. Usually no, occasionally one interdorsal thorn.

Individual tail thorns of males and females, up to ca. 5 mm long, consisting of a basal plate capped with a low enamelled crown which became lost in the specimens illustrated in Figures 4.5 and 5.5 (compare with Stehmann et al. [7]: fig. 13). Outline of well-rounded suboval basal plate longer than wide. Pulp cavity large and ventrally open. Alar thorns of male (Figure 4.1) up to ca. 8 mm long, strongly asymmetrical in dorsal view and curved along maximum extent. Crown positioned slightly posterior to the center of the basal plate,

with posteriorly curved, long and slender cusp lacking barb(s) (fractured in Figure 4.1). Basal plate anterior to crown longer than posterior part. Posterior part of basal plate unilaterally expanded, with strongly lobed basal lateral outline (Figure 4.1). Anterior part of basal plate elongated and tubular, tapering at the extremity to a sharp tip. Pulp cavity ventrally open in posterior part of the basal plate only.

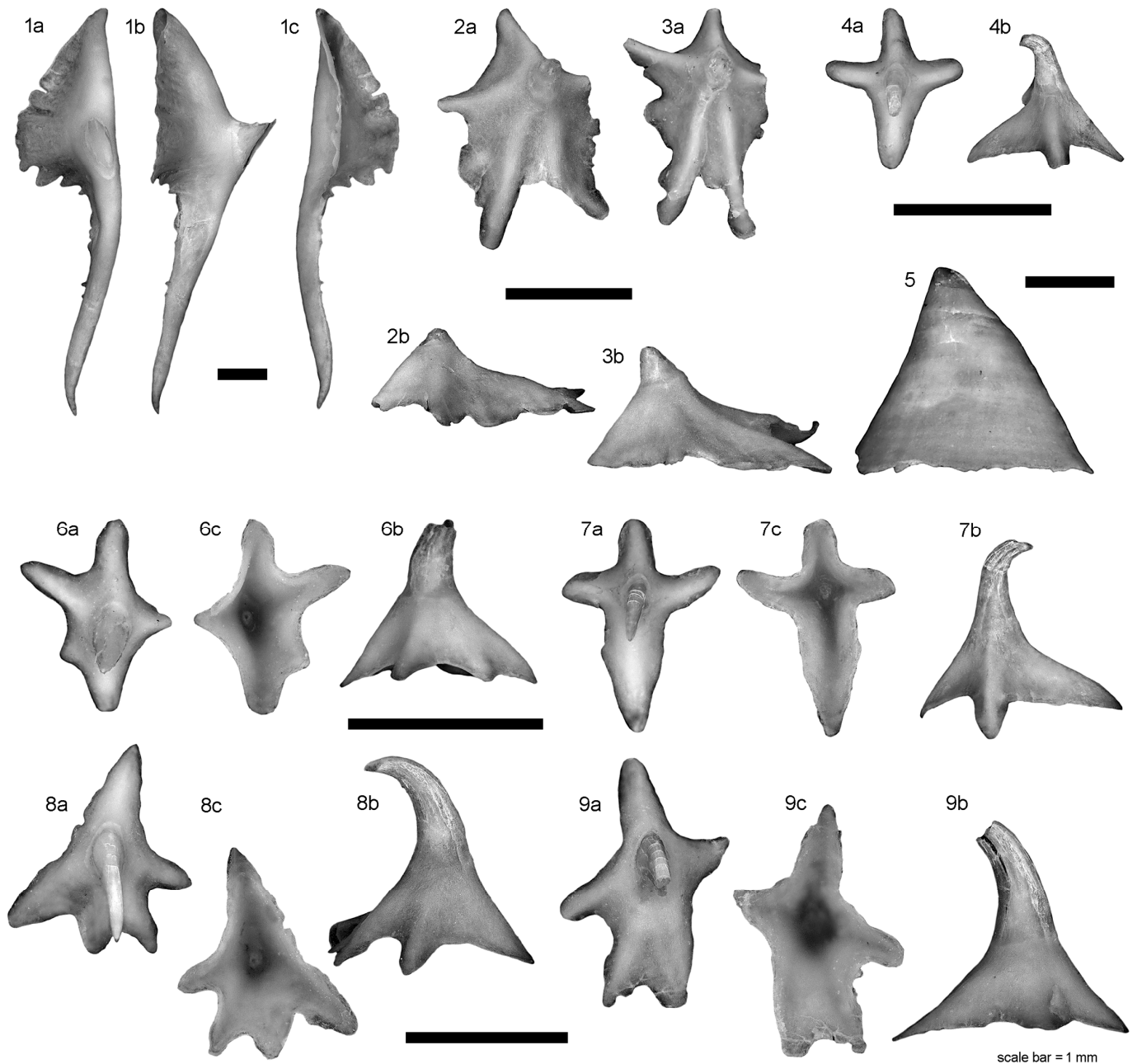


Figure 4. *Bathyraja arctowskii*, ZMH 115243, adult male, 502 mm TL. (1) alar thorn (AT) on right pectoral fin, H = ca. 2.3+ mm, Lmax = 7.8 mm; (2) enlarged denticle on right pectoral-fin apex (PAD), H = ca. 0.9+ mm, Lmax = 1.8 mm; (3) enlarged denticle on right pectoral-fin apex (PAD), H = ca. 0.7+ mm, Lmax = 1.7 mm; (4) scapular denticle on left shoulder (SD), H = ca. 0.7 mm, Lmax = 1.0 mm; (5) anterior median tail thorn (MTA), H = ca. 2.2 mm, L = 2.7 mm; (6) dorsolateral tail denticle (DTD) on anterior tail, H = ca. 0.8+ mm, Lmax = 1.0 mm; (7) dorsolateral tail denticle (DTD) on anterior tail, H = ca. 0.9+ mm, Lmax = 1.1 mm; (8) dorsolateral tail denticle (DTD) on midtail, H = ca. 1.2 mm, Lmax = 1.3 mm; (9) dorsolateral tail denticle (DTD) on midtail, H = ca. 1.3+ mm, Lmax = 1.5 mm. (1a–4a,6a–9a) = apical (dorsal) views; (1b–4b,5,6b–9b) = profile views; (1c,6c–9c) = basal (ventral) views.

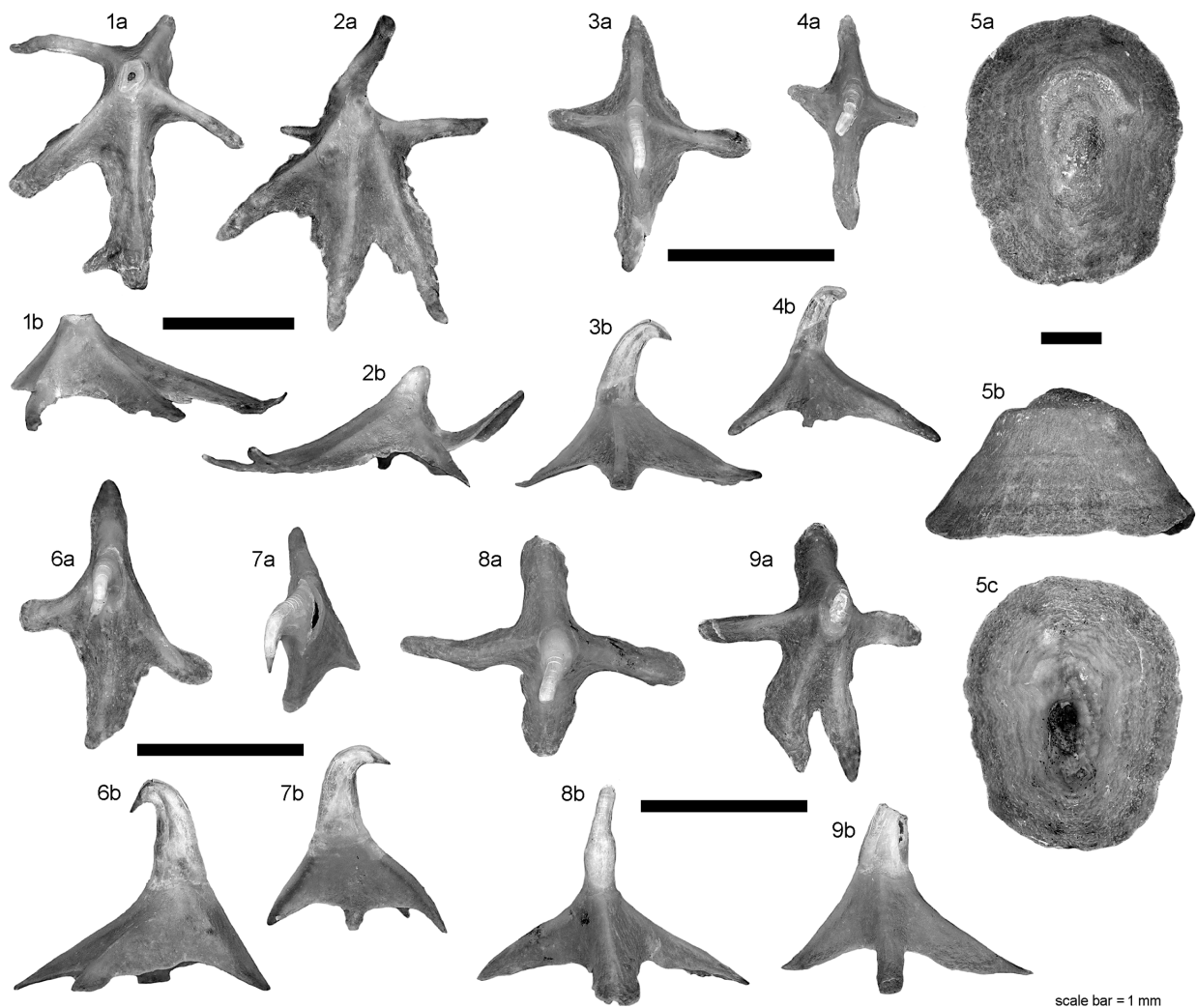


Figure 5. *Bathyraja arctowskii*, ZMH 115243, adult female, 510 mm TL. (1) enlarged denticle on right pectoral-fin apex (PAD), H = ca. 0.57+ mm, Lmax = 2.0 mm; (2) enlarged denticle on right pectoral-fin apex (PAD), H = ca. 0.64+ mm, Lmax = 2.4 mm; (3) scapular denticle on right shoulder (SD), H = ca. 1.0 mm, Lmax = 1.5 mm; (4) scapular denticle on right shoulder (SD), H = ca. 0.88 mm, Lmax = 1.3 mm; (5) anterior median tail thorn (MTA), H = ca. 2.4 mm, W = 3.5 mm, Lmax = 4.3 mm; (6) dorsolateral tail denticle (DTD) on anterior tail, H = ca. 1.5 mm, Lmax = 1.5 mm; (7) dorsolateral tail denticle (DTD) on anterior tail, H = ca. 1.1 mm, Lmax = 1.1 mm; (8) dorsolateral tail denticle (DTD) on midtail, H = ca. 1.1 mm, Lmax = 1.6 mm; (9) dorsolateral tail denticle (DTD) on midtail, H = ca. 1.2+ mm, Lmax = 1.9 mm. (1a–9a) = apical (dorsal) views; (1b–9b) = profile views; (5c) = basal (ventral) view.

The dorsal surface is almost completely and densely set with fine dermal denticles, including the caudal and dorsal fins, as well as partially the integument covering the eyeballs dorsally, but becomes more loosely set on pectoral centers and axils with growth. Posterior pelvic-fin lobes are smooth in most specimens, outer and inner surfaces of the clasper are completely smooth, like also the whole ventral surface.

Denticles in equivalent positions (SD, DTD, PAD in Figure 1) of males and females generally have similar or even the same morphologies and dimensions. Denticles from all sampled positions (except the alar thorns) are of the “spiny crown” type, whereas the “myrmecoid crown” type is absent (compare with fig. 2 in Gravendeel et al. [23]). In all denticles, the pulp cavity is ventrally open (Figure 4.6c–4.9c). Scapular denticles (SD, ca. 0.8–1.5 mm in diameter) typically belong to the “cross type” with four limbs (= “dorsal ridges”

of Gravendeel et al. [23]: fig. 3; Figures 4.4 and 5.4) or rarely the “star type” with five limbs of the basal plate. Dorsolateral tail denticles (DTD) tend to be slightly larger in dimensions than SD denticles, and have more variable shapes of the basal plate, ranging from three- to four-limbed (cross type) or to irregular five-limbed shapes (Figures 4.6–4.9 and 5.6–5.9). All SD and DTD denticles examined have a dome-shaped basal plate that merges apically into the upright lower crown and the strongly hooked cusp. The enamel-dentine junction typically occurs at the middle of the denticle’s height. In contrast to these, the PAD denticles have a low, five-limbed basal plate of the “leaf-type” or modified “star-type” and a low crown that appears to lack a hooked cusp (Figures 4.2–4.3 and 5.1–5.2). However, inspection of the PAD fields in the male shows that a low cusp was present in most of the denticles before abrasion. The thin dentine lamellae between the dorsal ridges may be irregularly widened and then show crenated to lobed edges.

Coloration. Dorsal ground color plain dark to medium greyish-brown, often with mostly indistinct scattered pale and dusky spots on disc, posterior pelvic lobes and on sides of tail, occasionally with transverse white pseudocellus-stripe on inner posterior pectorals. Underside mostly plain white or pale, often with grey marked cloaca and grey spots on belly to gill region, occasionally grey spotted posterior pectoral margins, origin and sides of tail, or tail partly dark.

Clasper external morphology. Clasper stem a solid rod of equal width, with the glans only little widening and short. The most obvious component of the dorsal lobe is a deep and long pseudosiphon (ps) along the outer margin extending over three fourths of glans length. A cleft (cf) is found in distal half of the glans between the axial cartilage ridge and the inner wall of dorsal lobe. A narrow cartilage rod is situated medially in proximal glans, the pseudorhipidion (pr), which covers proximally the axial cartilage (ax). The latter continues visible on deeper level as a ridge from underneath tip of pr to the extreme tip of the glans. Very prominent component on entire length of ventral lobe is the somewhat twisted and long projection (pj), a firm cartilage covered by integument and connected to outer ventral lobe margin with integument. A deep and wide sentina hollow (sn) underneath the pj and the integument spanning to outer ventral lobe margin runs out with its proximal wall as a narrow integument ridge diagonally across the axial cartilage to the proximal end of the cleft. Within the sentina, externally not visible, is the ax-blade-like tip of the sentinel (st) found as a sharp cutting tip edge of the at1 cartilage.

3.2.2. Skeletal Morphology

Clasper skeleton. Clasper terminal skeleton with distal processes of dorsal marginal cartilage (forming external pseudorhipidion) and ventral marginal cartilage (forming external projection), three dorsal terminal cartilages (with dt1 very large and encapsulating terminal skeleton), drop-shaped ventral terminal (not appearing as an external component) and one accessory terminal cartilage.

Cranium. Cranium with short, broadly bullet- or spearhead-shaped anterior fontanelle and elongated, narrowly triangular posterior fontanelle. Ovoid nasal capsules large and strongly forwardly inclined at a 54–75° angle of their straight rear edges to longitudinal axis of cranium. Orbital region evenly deeply concave; otic region broadly bulky, with short occipital condyles and small jugal arches not or hardly exceeding the contour of the occiput rearward or laterally. Snout supported by forward extension of pectoral propterygia and radials extended to nearly snout tip and rostral node. Rostral shaft length 44.5–53.8% of cranium total and 80.9–116.5% of nasobasal length; maximum ethmoidal width 45.1–56.9% of cranium total length, 95.8–103.7% of nasobasal length, 2.9–3.4 times minimum dorsal interorbital width, and 1.7–1.9 times maximum width of otic region. Anterior fontanelle length 18.7–38.9% of rostral shaft and 10.1–17.9% of cranium total length, its length 0.9–1.8 times its maximum width, and its tip hardly extending into rostral shaft length.

Pelvic girdle. Pelvic girdle with massive ischiopubic bar, anterior contour nearly straight, posterior contour slightly to deeply concave; prepelvic processes moderately long, solid, conical, and straight to somewhat inclined inwards, their length 3.2–4.4 times median

thickness of ischiopubic bar. Iliac processes massive and curving inwards, with broad, quadrangular tip. Each iliac region with two foramina.

Scapulocoracoid. Scapulocoracoid elongated rectangular in lateral view, with very asymmetrical anterior position of the mesocondyle. Overall shape and number, shape and arrangement of postdorsal and postventral foramina variable, but scapulocoracoid always with a solid horizontal anterior bridge separating the anterior fenestra into a smaller anterior dorsal and an anterior ventral fenestra. Overall shape moderately short to elongated rectangular, with rounded to sharply marked rear corner and nearly straight to deeply concave posterior margin sloping to the metacondyle. Anterior dorsal and ventral fenestrae large, postdorsal fenestrae large or a combination of a large anterior fenestra and several small foramina, postventral fenestrae mostly small and arranged in a chain along the ridge between meso- and metacondyle. Pre-mesocondyle length 25.6–38.0% of maximum length and 35.7–58.7% of post-mesocondyle length. Maximum length 1.3–1.6 times maximum height at scapular process. Height at rear corner 83.3–85.3% of maximum height. Combined height of both anterior fenestrae 37.4–43.3% of maximum height at scapular process and 26.8–28.8% of the element's maximum length.

Skeletal meristics. Trunk vertebrae (Vtr): 30–37; predorsal tail vertebrae (Vprd): 66–80; total predorsal vertebrae: 97–113; terminal tail vertebrae (Vterm, approximately): 23–40; total vertebrae (Vtotal, approximately): 120–151; pectoral radials, left: 70–89, right: 70–90; pelvic radials, left: 4+16–5+20, right: 4+17–5+19.

3.2.3. Egg Case Morphology

The description of the egg case morphology is based on the lectotype (IRSNB 25 [orig. 3005]) and paralectotypes (IRSNB 26 [orig. 3006] and IRSNB 27 [orig. 3007]), as well as two egg cases catalogued under ZMH 9014). Figure 6 shows the lectotype and paralectotype egg cases in dorsal and ventral views, Table 1 provides morphometrics of all five egg cases.

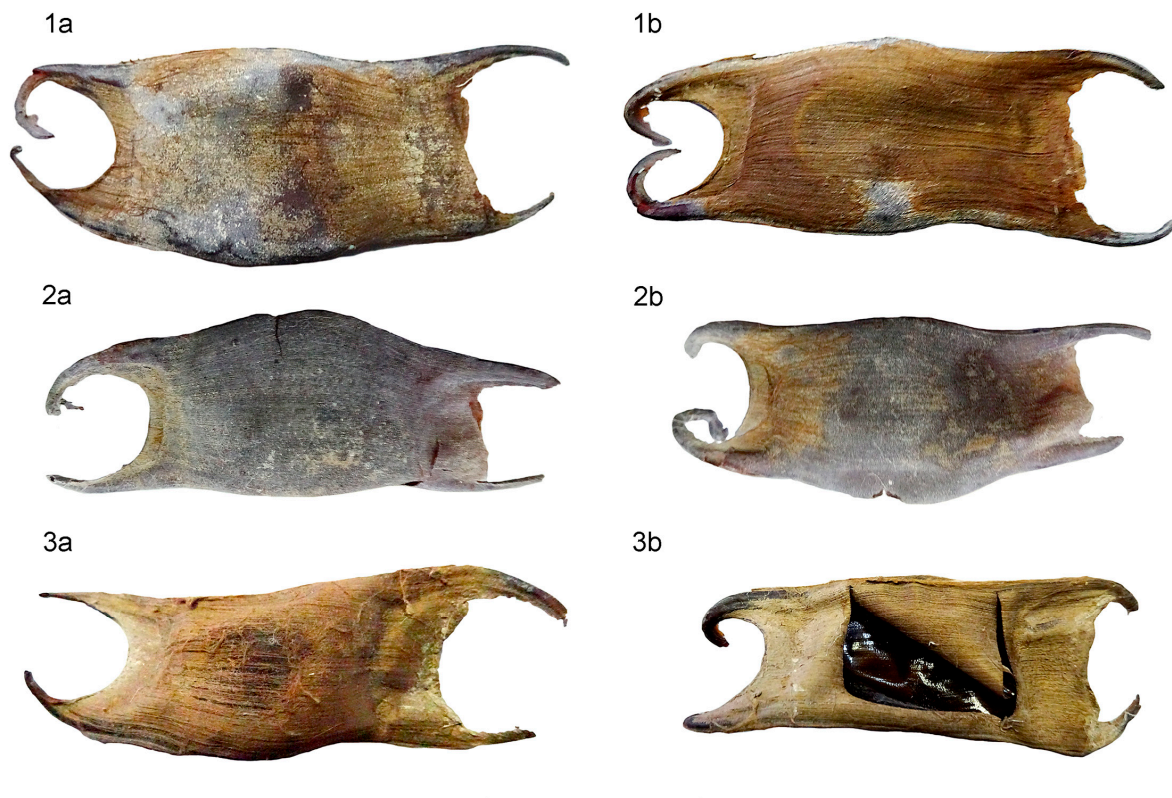


Figure 6. *Bathyraja arctowskii*, three empty egg cases, IRSNB, Brussels, Belgium. (1a,b) lectotype IRSNB 25; (2a,b) paralectotype IRSNB 26; (3a,b) paralectotype IRSNB 27. (1a–3a) dorsal views; (1b–3b) ventral views. Scale bar: 40 mm.

Table 1. *Bathyrāja arctowskii*, morphometrics of the lectotype IRSNB 25, the two paralectotypes IRSNB 26 and IRSNB 27, as well as two egg cases catalogued under ZMH 9014; all values are given in mm.

	ZMH 9014	ZMH 9014	IRSNB 25	IRSNB 26	IRSNB 27 *
	empty egg case	egg case with embryo	empty egg case	empty egg case	empty egg case
ECTL_1, egg case total length incl. length of bent horns (along curve)	141.5	146.4	>126.4 (d)	>118.1 (d)	>112.5 (d)
ECTL_2, egg case total length incl. horizontal length of bent horns	121.8	120.2	>105.9	>96.5	>99.5
ECL, egg case length; measured longitudinally between the anterior and posterior apron borders	77.6	76.1	67.5	64.3	62.6
AAL, anterior apron length	5.1	5.1	4.5	3.7	7.0
PAL, posterior apron length	12.6	12.9	15.6 (b)	10.5 (b)	15.1 *
ABW, anterior border width; distance between the bases of the anterior horns	20.1	20.0	22.9	19.4	23.0
PBW, posterior border width; distance between the bases of the posterior horns	21.0	21.1	23.8	20.5	24.8
MAW, maximum case width; transverse width of the case in its lateral plane at its widest part	42.3	40.7	42.1	37.4	32.1 *
MIW, minimum case width; transverse width of the case in its lateral plane at its narrowest part	34.5	34.4	34.4	31.1	32.9 *
LKW, lateral keel width; distance from the capsule keel junction to the keel edge	1.5	0.6	1.5 (a)	1.2 (a)	1.6 (a)
CBL, central body length (excl. aprons)	61.5	58.4	47.4 (e)	50.1 (e)	40.5 (e)
CBW, central body width (excl. lateral keels)	39.1	39.9	41.2	36.4	32.1 *
CH, Capsule height (maximum height)	18.9	18.9	14.1 (c)	17.6	>14.0 *
AHL_1, anterior horn length; distance from the horn base to the tips (along curve)	34.0	39.0	38.0	35.0	>30.0
PHL_1, posterior horn length; distance from the posterior horn base to the tips (along curve)	46.0	49.0	>41.0	>33.0	>42.0
AHL_2, anterior horn length; horizontal length between perpendicular lines	24.9	25.0	17.7	20.2	22.7
PHL_2, posterior horn length; horizontal length between perpendicular lines	37.5	34.5	33.9	25.9	32.2

Footer: Values marked with “>” are minimum values where horns of egg cases were partly broken off; * egg case IRSNB 27: body opened and strongly distorted; (a) lateral keel difficult to identify; measured values indicate widths of narrow lateral zones displaying a slightly different color than the body (in dry state); (b) posterior apron opened and damaged; (c) body of capsule impressed; (d) ECTL_1 = CBL + AHL + PHL; (e) CBL = ECL – AAL – PAL.

The lectotype and paralectotype egg cases generally correspond well with the two egg cases catalogued under ZMH 9014. Several differences can be ascribed to the generally worse condition of the types compared to the more recent egg cases at ZMH. Such damages are particularly found in the horns, leading to unnaturally small values in several measurements of the types (marked with “>”). Deviations due to the condition of egg cases are most pronounced in paralectotype IRSNB 27, which has the capsule body opened and strongly distorted. Apart from these artificial differences, all five egg cases agree well and only exhibit differences indicative of natural variation. The generally somewhat smaller values found in the type egg cases can be explained by shrinkage caused by the long-term storage of those egg cases. Skate egg cases are generally subject to shrinkage processes, Stehmann & Merrett [36], e.g., found a shrinkage between ~20–33% when comparing dry and wet egg cases of *B. richardsoni* (Garrick, 1961).

The egg cases of *B. arctowskii* are blackish-brown, the surface is smooth, with coverage of long, fine anchoring fibers. The aprons extend two-thirds onto the horns. The upper side of the egg case is strongly convex, the lower side moderately convex. The cross-section (anterior and posterior horns) is depressed. The length of the egg cases is about 120 mm including the horizontally measured length of the bent horns and ~63–78 mm measured longitudinally between the anterior and posterior apron borders. The latter

measurement is likely influenced by shrinkage in the three type egg cases (62.6–67.5 mm) and the fresh measurement is probably closer to the measurements of the two non-type egg cases (76.1–77.6 mm). The maximum case width (MAW), measured as the transverse case width in its lateral plane at its widest part, is ~37.4–42.3 mm and ~54–62% of egg case length (ECL). Again, the values of the type egg cases tend to be smaller possibly due to shrinkage and the measurements of paralectotype IRSNB 27 have been excluded due to its strong distortion. Lateral keels very narrow, ~2–4% of MAW. Anterior apron border broad, deeply concave. Posterior apron nearly straight, broad, and transverse. Anterior border width similar to that of posterior one, but posterior apron ~2.5–3.5 times longer than anterior one. Anterior horns short, their length along the curve (AHL₁) ~44–56% of ECL, curved inwards, tapering towards tips, becoming thin and filamentous. Posterior horns short but ~1.3–1.4 times longer than anterior ones and ~59–64% of ECL, curved inwards, tapering towards tips with tendrils coiling towards filamentous tips.

3.2.4. Ontogenetic Changes and Sexual Dimorphism

Bathyraja arctowskii shows pronounced ontogenetic changes and sexual dimorphism (Figure 7). As typical for skates, adult males have strongly undulated disc margins showing concavity at anterior sides of snout and at level of nape (vs. not to slightly undulated in females and juvenile males), alar thorns are present, and the teeth have longer cusps and are arranged in parallel rows (vs. quincunx pavement pattern).



Figure 7. *Bathyraja arctowskii*, egg case and different maturity stages, clockwise from bottom right to top right: empty egg case, 77.6 mm long, ZMH 9014; near-term male embryo, 120 mm total length (TL), ZMH 9014; juvenile female, 236 mm TL, ZMH 121822; subadult male, 424 mm TL, ZMH 121822; adult male, 533 mm TL, ZMH 120216. Scale bar: 5 cm.

Sexual dimorphism is particularly pronounced in the skeleton with the pelvic girdle being narrower with deeply (vs. slightly) concave posterior contour of ischiopubic bar as also typical for skates. Accordingly, the maximum width of the shoulder girdle and the maximum width of the pelvic girdle show sexual dimorphism, with dimorphism of shoulder girdle maximum width evidenced by ratio shoulder girdle maximum width/dorsal interorbital width (4.0–4.5 in males vs. ~5.4 in females) and dimorphism of pelvic girdle shown by ratio maximum

width of shoulder girdle/maximum width of pelvic girdle (1.4–1.5 vs. ~1.8). As typical for members of the genus *Bathyraja*, the degree of intraspecific variation of scapulocoracoid features is very high, referable to sexual dimorphism in the scapulocoracoid's overall shape and pronounced intraspecific natural variation in the number, shape and arrangement of postdorsal and postventral foramina, the latter probably being influenced by ontogenetic changes. The sexual dimorphism in the scapulocoracoid's general appearance is reflected in differences in the pre-mesocondyle length (~38.0% of maximum length in males vs. ~25.6% in females and ~58.7% vs. ~35.7% of post-mesocondyle length) and the ratio maximum length/maximum height at scapular process (~1.3 vs. ~1.6).

Apart from these differences, a very high number of ontogenetic changes can be found in *B. arctowskii*, including median tail thorns that become smaller and more widely spaced posteriorly in subadults and adults and are generally wider-spaced in large juveniles to adults as compared to small juveniles. Furthermore, the disc of embryos is narrower with disc width only ~51.7% TL (vs. 61.3–66.0% TL), the head is longer in larger specimens (dorsal length 17.6–21.6% TL in subadults and adults vs. 16.8–18.7% TL in juveniles vs. ~14.2% TL in embryos; ventral length 25.0–28.0% TL vs. 21.5–25.9% TL vs. not measurable), the snout is more acutely angled (snout angle 110–120° vs. 125–133° vs. ~140°) and proportionally longer (preorbital length 11.4–16.2% TL vs. 9.6–11.6% TL vs. ~8.1% TL and 3.7–5.3 vs. 2.5–3.6 vs. ~2.2 times interorbital width; preoral length 11.1–15.2% TL vs. 9.0–11.3% TL vs. ~8.8% TL; prenasal length 9.1–12.9% TL vs. 7.4–9.4% TL vs. ~7.4% TL), the eyes are smaller (orbit horizontal diameter 4.1–4.8% TL vs. 4.6–5.8% TL vs. ~5.4% TL; eyeball horizontal diameter 3.4–3.7% TL vs. 3.9–4.6% TL vs. ~4.4% TL), the spiracles are positioned closer together (interspiracular width 7.0–7.9% TL vs. 7.9–8.8% TL vs. ~8.7% TL), the nasal curtain is longer (length 3.4–4.1% TL vs. 2.8–3.4% TL vs. ~2.4% TL) and its lobes are set farther apart (interspace 4.0–5.3% TL vs. 2.8–4.0% TL vs. ~3.3% TL), the tail is wider and lower (tail height at pelvic tips 2.0–2.2% TL vs. 2.3–3.0% TL vs. ~4.3% TL; tail width 1.5–1.8 times vs. 1.1–1.5 times vs. ~1.1 times height at pelvic tips; tail height at first dorsal-fin origin 0.7–0.9% TL vs. 0.9–1.3% TL vs. ~1.3% TL; tail width 1.7–2.6 times vs. 1.1–1.8 times vs. ~1.4 times height at first dorsal-fin origin) and has longer lateral folds (length 44.3–47.7% TL vs. 35.0–47.6% TL vs. ~32.8% TL and along full tail length vs. along posterior two thirds to almost full length vs. along posterior two thirds), the trunk is longer (snout tip to mid-cloaca 45.6–49.6% TL vs. 41.9–45.6% TL vs. ~41.3% TL; snout tip to first hemal spine 48.0–51.5% TL vs. 43.8–48.2% TL vs. not measurable), and the tail is shorter (mid-cloaca to first dorsal-fin origin 38.4–42.8% TL vs. 44.1–46.4% TL vs. ~46.7% TL; mid-cloaca to second dorsal-fin origin 42.5–47.4% TL vs. 48.2–50.4% TL vs. ~52.3% TL; mid-cloaca to tail tip 49.4–52.7% TL vs. 53.2–59.3% TL vs. ~60.2% TL; mid-cloaca to tail tip 1.0–1.2 times vs. 1.2–1.4 times vs. ~1.5 times snout tip to mid-cloaca). Additionally, the dorsal dermal denticle coverage becomes more loosely set on pectoral centers and axils with growth and the dorsal color pattern of light dots and streaks is generally more pronounced in small specimens albeit variable individually. Intraspecific variation in color pattern has been reported regularly within the Arhynchobatidae (see, e.g., Weigmann [6]).

3.2.5. Size and Maturity

Bathyraja arctowskii is the smallest known species of the genus, attaining about 61 cm TL based on a 61 cm TL specimen from the Ross Sea (NMNZ P.037551), maturing around 36–50 cm TL (based on the largest examined juvenile male of 38.4 cm TL, examined subadult males from 36.1–45.0 cm TL, examined late subadult males from 46.1–49.5 cm TL, and the smallest examined adult male of 49.0 cm TL), hatching at about 12–13 cm TL (based on male embryo ZMH 9014 and the smallest juvenile female examined in detail and catalogued under ZMH 121822), and laying egg cases 6.3–7.8 cm long and 3.7–4.2 cm wide (based on the three types and non-type egg cases examined).

3.2.6. Distribution

Bathyraja arctowskii appears to be a circum-Antarctic species, with its center of distribution in the Atlantic sector of the Southern Ocean. It is known from off the South Shetland, Brabant,

and Biscoe Islands to the South-East Weddell Sea, from the Ross Sea in the Pacific sector, and two specimens from Prydz Bay in the Indian Ocean sector of the Southern Ocean. The known depth distribution is 0–1685 m but the species is mainly found between 126 and 810 m depth based on 270 specimens examined in the ZMH collection. Records shallower than that are based only on one lot with six specimens from 0–140 m depth (ZMH 120223) and records deeper than 810 m depth are based solely on 61 specimens from the NMNZ collection. So far, no maturity-related differences in preferred depth areas have been detected, with both juveniles and adults occurring in shallower as well as deeper zones of the known depth range.

4. Discussion

4.1. Dental Morphology

The dental morphology of adult males and/or females of *Bathyraja* spp. and *Rhinoraja* spp. has been previously documented to varying degrees for the following species: *B. albomaculata* (Norman, 1937), *B. griseocauda* (Norman, 1937), *Rhinoraja longicauda* Ishiyama, 1952, *B. macloviana* (Norman, 1937), *B. richardsoni* (Garrick, 1961), *B. spinicauda* (Jensen, 1914) and *B. taranetzi* Dolganov, 1983 [37–43]. Several other studies presented merely general views of the ventral side or a close-up of the oronasal region, which do not allow the closer interspecific comparison of dental characters (e.g., [7,44–48]).

The abovementioned species of *Bathyraja* and *Rhinoraja*, including *B. arctowskii* (this study), have in common the following characteristics of male and female teeth: Absence of dignathic heterodonty; moderately high to high root (with respect to crown height); holaulacorhize vascularization with deep nutritive groove and often one large, sub-central foramen; well-separated root lobes that markedly diverge basally at lateral, labial and lingual sides of the root; and in adult male teeth, a more or less high crown with a lingually strongly inclined cusp and commonly rather long cutting edges on the transverse ridge.

On the other hand, there are some tooth characteristics that differ from species to species and could become diagnostic for particular species or species-groups, as tooth characteristics will become better known within *Bathyraja* spp. Male/female teeth of *B. richardsoni* (Herman et al. [41]: pl. 7–8; Garrick [38]: text-fig. 1d) have a narrower crown (base) and a much more elongated cusp with a convex labial surface, and a narrower, more pointed uvula than adult male teeth of probably all other species listed above, including *B. arctowskii* (Figure 2). A quite large, sub-circular crown base, combined with a narrow cusp equipped with convex labial surface, is observed in males (and females due to weak sexual heterodonty; see below) of *B. spinicauda* (Herman et al. [40]: pls. 7–10) and probably in *B. taranetzi* (Raschi & McEachran [39]: fig. 5a,b) and *B. griseocauda* (Sáez & Lamilla [42]: fig. 1b,c), whereas males of the other examined species (except *B. richardsoni*; see above), i.e., *B. albomaculata*, *B. arctowskii*, *B. macloviana* and *Rhinoraja longicauda*, have basally broader, more triangular cusps with a nearly flat labial surface (Herman et al. [40]: pl. 1–4; fig. 2; Scenna et al. [43]: fig. 6; Herman et al. [41]: pl. 40). Latero-basally widened root lobes, clearly wider than the lateral crown base, are typically present in species with a high, cuspidate crown in anterior to posterior tooth files, i.e., *B. richardsoni* and partly in *B. albomaculata*, *B. spinicauda*, *R. longicauda* and perhaps in *B. griseocauda*, but they tend to be narrower in *B. arctowskii* and *B. macloviana*.

Finally, the extent of sexual heterodonty differs markedly between the few species of *Bathyraja* yet examined in detail. In *B. arctowskii*, the crown height of anterior teeth in the mature male (Figure 2) is estimated to be three to four times higher (in profile view) than in the corresponding teeth of the mature female, which indicates distinct sexual heterodonty (Figure 3). Moderate to distinct forms of sexual heterodonty have also been shown for *B. macloviana* (Scenna et al. [43]: fig. 6), *B. taranetzi* (Raschi & McEachran [39]: p. 1895, fig. 5a,b), *B. spinicauda* (Herman et al. [40]: pls. 7–10) and *B. albomaculata* (Herman et al. [40]: pls. 1–4). Notably, the teeth of a mature female of *B. spinicauda* have a clearly cuspid shape (i.e., “male” morphology), being at first sight almost indistinguishable from the teeth of a mature male but differing from male teeth by the overall slightly lower cusp height [40].

By contrast, females and males of *B. griseocauda* have been reported to be sexually homodont (or nearly so) and thus have almost identical crown morphologies in equivalent

mature male and female tooth files [42]. Similarly, *B. richardsoni* shows minor differences in tooth shape between an adult male (Herman et al. [40]: pls. 7–8, 180 cm TL) and adult female (Garrick [38]: text-fig. 1d,e (drawings), 133.1 cm TL). However, female individuals of this species need to be reexamined to assess apparent homodonty.

In summary, we note that of the few species with well-characterized dentition and single teeth, *B. arctowskii*, *B. albomaculata* and perhaps *B. macloviana* appear to be the most similar in dental morphology. Like *B. arctowskii*, the other two species are only present in the Southern Hemisphere but are geographically more restricted to the Southeast Pacific and the Southwest Atlantic, from Chile to Argentina and the Falkland Islands [2].

4.2. Morphology of Dermal Denticles and Thorns

The morphology of the dermal denticles and thorns of *Bathyraja* spp. and *Rhinoraja* spp. has previously been documented to varying degrees for several species. However, the morphological details of the basal plate edges and the pulp cavity are concealed when the denticles are still imbedded in the skin (Figure 8, and Stehmann et al. [7]: fig. 12, for alar thorns). Although the use of untreated skin samples for illustrating dermal denticle morphology is common in the literature (e.g., [24,48–51]) and saves a lot of preparation time, the basal plates of the dermal denticles cannot be shown to their full extent (Figure 8 vs. Figures 4 and 5). Therefore, denticles should be isolated using physico-chemical methods before their closer characterization. This has previously been carried out in only a few studies on dermal denticles (including alar and tail thorns) of *Bathyraja* spp. by Raschi & McEachran [39] [*B. taranetzi* Dolganov, 1983], McEachran & Konstantinou [52] [nine species of *Bathyraja* and *Rhinoraja*], Henderson et al. [53] [*B. albomaculata* (Norman, 1937)], Gallagher et al. [54] [*B. brachyurops* (Fowler, 1910)], and Iglésias & Lévy-Hartmann [47] [*B. leucomelanos* Iglésias & Lévy-Hartmann, 2012].

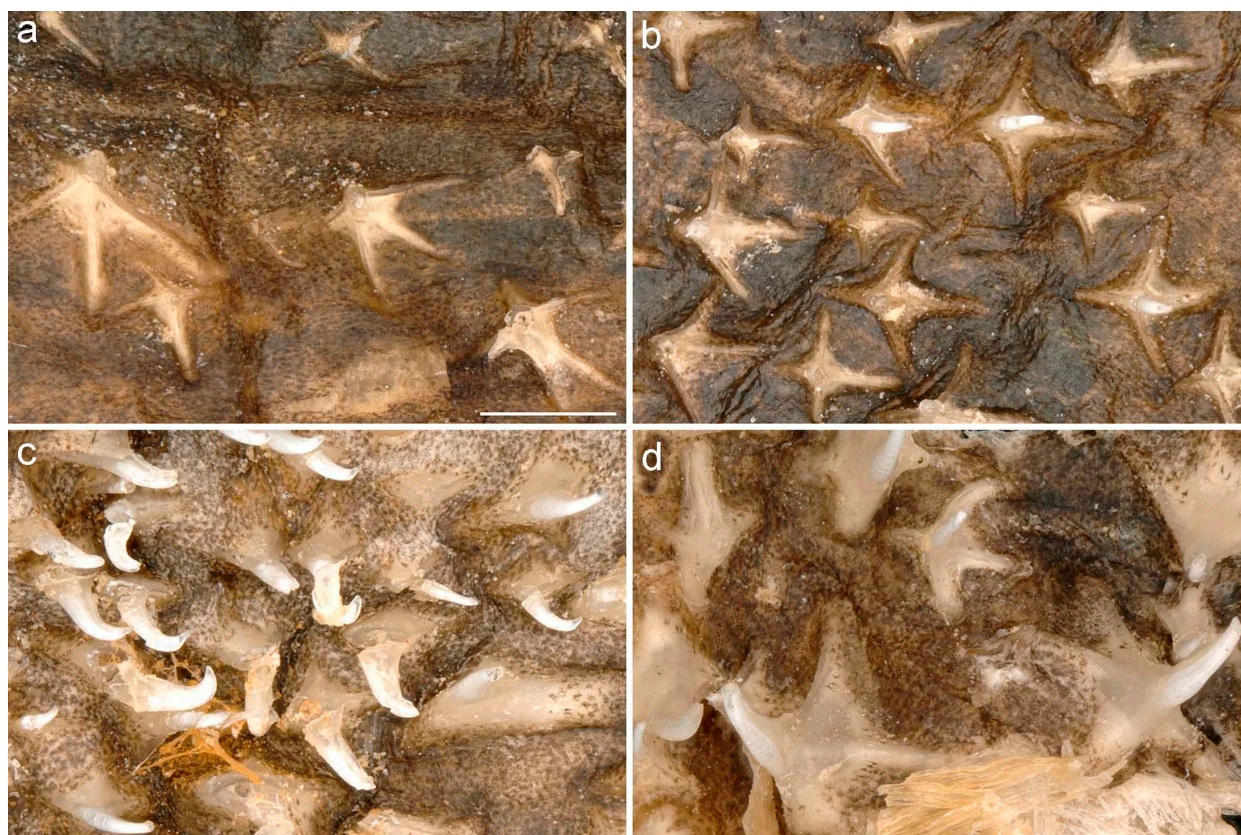


Figure 8. *Bathyraja arctowskii*, ZMH 115243, adult female, 510 mm TL. (a) enlarged denticles on right pectoral-fin apex (PAD), (b) scapular denticles (SD) on right shoulder, (c) dorsolateral tail denticles (DTD) on anterior tail, (d) dorsolateral tail denticles (DTD) on midtail. Scale bar (a–d): 1 mm. Note limited informative value as compared to images of dissected and cleaned dermal denticles in Figures 4 and 5.

The median caudal thorns of *B. arctowskii* (Figures 4.5 and 5.5) are much like the corresponding tail thorns of *B. albomaculata* (Henderson et al. [53]: fig. 1), *B. brachyurops* (Gallagher et al. [54]: fig. 3), *B. kincaidii* (Perez et al. [55]: fig. 1) and probably *B. taranetzi* (Raschi & McEachran [39]: fig. 4b) in the broad, cone-shaped basal plate, whereas the caudal thorns of *B. leucomelanos* seem to be mesio-distally more compressed (Iglésias & Lévy-Hartmann [47]: figs. 5 and 7). The annual growth rings are indistinct in the unstained thorns of *B. arctowskii* (Figures 4.5 and 5.5). In the median thorns of *B. leucomelanos*, *B. kincaidii* and *B. albomaculata*, the oblique walls forming the basal plate are moderately to strongly folded perpendicular to the growth rings, which is not observed in *B. arctowskii*. For the female type specimen of *B. richardsoni*, Garrick ([38]: 743–744, fig. 1g) reported the lack of large, raised thorns on the median tail but instead found “ovoid cutaneous structures, ca. 12–15 mm long, scarcely raised from the surface and somewhat scar-like in appearance”. Whether these structures are pathologic in origin or represent a specific characteristic of *B. richardsoni* still has to be examined.

As with all species of *Bathyraja* ([52]: 167; [50]: 162), malar thorns are not present in *B. arctowskii*. The occurrence and characteristics of alar (and malar) thorns in several supra-specific taxa of extant skates have been extensively examined and described by McEachran & Konstantinou [52], but only few alar thorns specific to *Bathyraja* spp. have been illustrated. Nonetheless, the morphological characteristics of alar thorns in our male specimen of *B. arctowskii* are very similar to those shown in two species of *Bathyraja* by McEachran & Konstantinou ([52]: fig. 10a [*B. kincaidii*]) and Raschi & McEachran ([39]: fig. 4c,d [*B. taranetzi*]).

Deynat [56] studied numerous species of *Bathyraja* (see Deynat & Séret [49]: appendix; without *B. arctowskii*) for their dermal denticles and states that “the denticles are varying in size depending on the species” and “the morphology of the denticles remains constant regardless of their position on the body surface and the (ontogenetic) developmental stage considered” [56]. We largely confirm these observations for males and females of *B. arctowskii*, with the exception that the denticle size and the shape of basal plates clearly differs between general dorsal denticles (i.e., scapular, SD, and dorsolateral tail, DTD) and enlarged denticles of the pectoral-fin apex (PAD). Whether these specific differences also exist in other species of *Bathyraja* and have been overlooked due to lack of preparation of isolated specimens cannot be verified at present.

With respect to the morphological details of general small denticles (SD, DTD) in *B. arctowskii* (Figures 4.4,6–9 and 5.3,4,6–9), we find a close correspondence with the denticles of many species from the Northeast and Northwest Pacific, New Caledonia, and off Antarctica (denticles from the midpectoral dorsal surface, anterior pectoral fins, dorsal fins and head region behind the eyes; e.g., Raschi & McEachran [39]: fig. 3a–c; Deynat [56]: pl. 19, fig. b–d; Iglésias & Lévy-Hartmann [47]: fig. 6; Knuckey & Ebert [48]: figs. 4,9,15,22 and 34). Minor differences refer mainly to the length of the crown relative to the basal plate, the curvature of the posteriorly recurved cusp and/or the presence of a hooked apex, and the number and regularity of limbs (points) at the cross-shaped to stellate basal plate. The latter commonly vary in number from three to five, in some species to six or seven, with possible differences in numbers existing between some species [48].

4.3. Conservation Implications

There is no directed fishery for *Bathyraja* spp. in the Southern Ocean, but most species are regularly taken as bycatch in bottom trawl fisheries. Their commercial exploitation on a moderate level can be expected [8]. *Bathyraja eatonii* is exploited commercially by trawler fisheries in Kerguelen waters and constitutes frequent bycatch in the toothfish and icefish fisheries [8,34,57]. *Bathyraja irrasa* is also a frequent bycatch of toothfish and icefish fisheries [57]. *Bathyraja maccaini*, the most abundant large species of *Bathyraja* in the Southern Ocean, is regularly taken as bycatch in bottom trawl hauls and probably utilized for fishmeal [8]. *Bathyraja meridionalis* is regular bycatch of longline fisheries for Patagonian Toothfish around the Falkland Islands [8], and *B. murrayi* is frequently taken in

commercial bottom trawl hauls for Antarctic cod, toothfish and icefish [34,57], but probably not commercially harvested due to its small size [8]. *Bathyraja arctowskii* has been reported as incidental catch in demersal trawl and longline fisheries, including fisheries targeting toothfish (*Dissostichus* spp.) [58]. Although the effect of fishing, if any, on the species is unknown, it appears to be rather common locally, at least in the Atlantic sector of the Southern Ocean, with up to 94 juvenile to subadult specimens caught in one single haul [7]. Furthermore, the species has a widespread, circum-Antarctic range covering the Atlantic, Pacific and Indian Ocean sectors of the Southern Ocean [7] and is not suspected to have declined to a level approaching the population reduction threshold [58]. Considering its commonness and its wide-ranging distribution that lies entirely within the Commission for the Conservation of Antarctic Marine Living Resources (CCAMLR) Convention Area, where fisheries management measures including bycatch limits and fishing depth restrictions are implemented and likely offer the species some refuge, *B. arctowskii* was assessed as Least Concern based on the International Union for Conservation of Nature (IUCN) Red List of Threatened Species categories [58]. Fisheries in this area are regulated by a multi-species bycatch limit of 120 t for all “skates and rays”, species-specific bycatch is recorded, all skates must be released alive (and may only be retained if hauled dead), and a move-on-rule is applied if more than 1 t of skate/ray are caught in one haul, not permitting vessels to fish within 5 nautical miles of the location for at least five days [58]. Furthermore, demersal fishing for toothfish (*Dissostichus* spp.) is only permitted below depths of 550 m in CCAMLR waters [59], offering the species some refuge in the shallow part of its depth range. In addition, *B. arctowskii* appears to be common in the Ross Sea [7,8], where the Ross Sea Region Marine Protected Area (RSRMPA) was introduced in 2016, prohibiting fishery activities in most parts, with only a few exceptions that must be conducted in accordance with other CCAMLR conservation measures [60]. Nevertheless, further information is required on the population status, ecology and life history, as well as interactions with fisheries, including post-release mortality. *Bathyraja arctowskii* could be at risk in the future if fisheries expand their reach into deeper waters [58].

Author Contributions: Conceptualization, S.W.; methodology, S.W. and T.R.; software, S.W. and T.R.; validation, S.W. and T.R.; formal analysis, S.W. and T.R.; investigation, S.W. and T.R.; resources, S.W. and T.R.; data curation, S.W.; writing—original draft preparation, S.W.; writing—review and editing, S.W. and T.R.; visualization, S.W. and T.R.; supervision, S.W.; project administration, S.W.; funding acquisition, S.W. All authors have read and agreed to the published version of the manuscript.

Funding: This research received no external funding.

Institutional Review Board Statement: Not applicable.

Data Availability Statement: The data presented in this study are available in this published article.

Acknowledgments: The authors are very grateful to Ralf Thiel (ZMH) for granting access to and loan of specimens in the ZMH collection for examinations and access to the photo- and radiography facilities at ZMH, as well as for approving the dissections of the disintegrated specimens, and to Irina Eidus and Thilo Weddehage (ZMH) for their help with the radiography, collection database and cards, as well as for providing photographs of several specimens. The authors are also very grateful to Olivier Pauwels (IRSNB) for granting access to the syntype egg cases in the IRSNB collection for examinations, to Andrew Stewart and Carl Struthers (NMNZ) for detailed data and photographs of specimens at NMNZ, and to Jürgen Pollerspöck (Shark-References) and William T. White (CSIRO) for providing references. The authors are grateful to the journal editors and reviewers of the manuscript for their helpful comments.

Conflicts of Interest: The authors declare no conflict of interest.

References

1. Last, P.R.; Séret, B.; Stehmann, M.F.W.; Weigmann, S. Skates, family Rajidae. In *Rays of the World*; Last, P.R., White, W.T., de Carvalho, M.R., Séret, B., Stehmann, M.F.W., Naylor, G.J.P., Eds.; CSIRO Publishing: Melbourne, Australia, 2016; pp. 204–363.
2. Last, P.R.; Stehmann, M.F.W.; Séret, B.; Weigmann, S. Softnose skates, family Arhynchobatidae. In *Rays of the World*; Last, P.R., White, W.T., de Carvalho, M.R., Séret, B., Stehmann, M.F.W., Naylor, G.J.P., Eds.; CSIRO Publishing: Melbourne, Australia, 2016; pp. 364–472.
3. Séret, B.; Last, P.R.; Weigmann, S.; Stehmann, M.F.W. Legskates, family Anacanthobatidae. In *Rays of the World*; Last, P.R., White, W.T., de Carvalho, M.R., Séret, B., Stehmann, M.F.W., Naylor, G.J.P., Eds.; CSIRO Publishing: Melbourne, Australia, 2016; pp. 494–508.
4. Weigmann, S.; Séret, B.; Last, P.R.; McEachran, J.D. Pygmy skates, family Gurgesiellidae. In *Rays of the World*; Last, P.R., White, W.T., de Carvalho, M.R., Séret, B., Stehmann, M.F.W., Naylor, G.J.P., Eds.; CSIRO Publishing: Melbourne, Australia, 2016; pp. 473–493.
5. Weigmann, S. Annotated checklist of the living sharks, batoids and chimaeras (Chondrichthyes) of the world, with a focus on biogeographical diversity. *J. Fish Biol.* **2016**, *88*, 837–1037. [[CrossRef](#)]
6. Weigmann, S. Reply to Borsa (2017): Comment on ‘Annotated checklist of the living sharks, batoids and chimaeras (Chondrichthyes) of the world, with a focus on biogeographical diversity by Weigmann (2016)’: Reply to borsa’s comment on weigmann (2016). *J. Fish Biol.* **2017**, *90*, 1176–1181. [[CrossRef](#)]
7. Stehmann, M.F.W.; Weigmann, S.; Naylor, G.J.P. First complete description of the dark-mouth skate *Raja arctowskii* Dollo, 1904 from Antarctic waters, assigned to the genus *Bathyraja* (Elasmobranchii, Rajiformes, Arhynchobatidae). *Mar. Biodivers.* **2021**, *51*, 18. [[CrossRef](#)]
8. Weigmann, S.; Stehmann, M.F.W.; Bürkel, D.L. Family Arhynchobatidae—Softnose skates. In *Fishes of the Southern Ocean, Revised Edition*; Gon, O., Gon, J., Eds.; SAIAB: Makhanda, South Africa, *in press*.
9. Stehmann, M. Notes on the Systematics of the Rajid Genus *Bathyraja* and its Distribution in the World Oceans. In *Indo-Pacific Fish Biology: Proceedings of the Second International Conference on Indo-Pacific Fishes*; Uyeno, T., Arai, R., Taniuchi, T., Matsuura, K., Eds.; Ichthyological Society of Japan: Tokyo, Japan, 1986; pp. 261–268.
10. Dollo, L. *Poissons. Expédition Antarctique Belge, Résultats du Voyage du S.Y. “Belgica” en 1897-1898-1899, Rapports Scientifiques*; J.-E. Buschmann: Antwerpen, Belgium, 1904.
11. Bigelow, H.B.; Schroeder, W.C. Notes on a small collection of rajids from the sub-Antarctic region. *Limnol. Oceanogr.* **1965**, *10*, R38–R49. [[CrossRef](#)]
12. Springer, S. Three species of skates (Rajidae) from the continental waters of Antarctica. In *Biology of the Antarctic Seas IV*; Llano, G.A., Wallen, I.E., Eds.; American Geophysical Union: Washington, DC, USA, 1971; Volume 17, pp. 1–10.
13. Treloar, M.A.; Laurenson, L.J.B.; Stevens, J.D. Descriptions of rajid egg cases from southeastern Australian waters. *Zootaxa* **2006**, *1231*, 53–68. [[CrossRef](#)]
14. Ebert, D.A.; Davis, C.D. Descriptions of skate egg cases (Chondrichthyes: Rajiformes: Rajoidei) from the eastern North Pacific. *Zootaxa* **2007**, *1393*, 1–18. [[CrossRef](#)]
15. Concha, F.; Hernández, S.; Oddone, M.C. Egg capsules of the raspthorn sand skate, *Psammobatis scobina* (Philippi, 1857) (Rajiformes, Rajidae). *Rev. Biol. Mar. Oceanogr.* **2009**, *44*, 253–256. [[CrossRef](#)]
16. Concha, F.; Oddone, M.C.; Bustamante, C.; Morales, N. Egg capsules of the yellownose skate *Zearaja chilensis* (Guichenot 1848) and the roughskin skate *Dipturus trachyderma* (Kreffft and Stehmann 1974) (Rajiformes: Rajidae) from the south-eastern Pacific Ocean. *Ichthyol. Res.* **2012**, *59*, 323–327. [[CrossRef](#)]
17. Ishihara, H.; Treloar, M.; Bor, P.H.F.; Senou, H.; Jeong, C.H. The comparative morphology of skate egg capsules (Chondrichthyes: Elasmobranchii: Rajiformes). *Bull. Kanagawa Prefect. Mus. Nat. Sci.* **2012**, *41*, 9–25.
18. Stehmann, M.F.W. Proposal of a maturity stages scale for oviparous and viviparous cartilaginous fishes (Pisces, Chondrichthyes). *Arch. Fish. Mar. Res.* **2002**, *50*, 23–48.
19. Henderson, A.C.; Arkhipkin, A.I. Maturity index validation in the white-spotted skate *Bathyraja albomaculata*, from the Falkland Islands. *J. Mar. Biol. Ass.* **2010**, *90*, 1015–1018. [[CrossRef](#)]
20. Ward, D.J. Additions to the fish fauna of the English Palaeogene. 5. A new species of *Raja* from the London Clay. *Tert. Res.* **1984**, *6*, 65–68.
21. Herman, J.; Hovestadt-Euler, M.; Hovestadt, D.C.; Stehmann, M. Contributions to the study of the comparative morphology of teeth and other relevant ichthyodorulites in living supraspecific taxa of chondrichthyan fishes. Part B: Batomorphii No. 1a: Order: Rajoidei—Family: Rajidae Genera and Subgenera: *Anacanthobatis* (*Schroederobatis*), *Anacanthobatis* (*Springeria*), *Breviraja*, *Dactylobatus*, *Gurgesiella* (*Gurgesiella*), *Gurgesiella* (*Fenestraraja*), *Malacoraja*, *Neoraja* and *Pavoraja*. *Bull. Inst. R. Sci. Nat. Belg.* **1994**, *64*, 165–207.
22. Cappetta, H. *Handbook of Paleoichthyology, Vol. 3E: Chondrichthyes. Mesozoic and Cenozoic Elasmobranchii: Teeth*; Dr. F. Pfeil: München, Germany, 2012.
23. Gravendeel, R.; Van Neer, W.; Brinkhuizen, D. An identification key for dermal denticles of Rajidae from the North Sea. *Int. J. Osteoarchaeol.* **2002**, *12*, 420–441. [[CrossRef](#)]
24. Bustamante, C.; Lamilla, J.; Concha, F.; Ebert, D.A.; Bennett, M.B. Morphological Characters of the Thickbody Skate *Amblyraja frerichsi* (Kreffft 1968) (Rajiformes: Rajidae), with Notes on Its Biology. *PLoS ONE* **2012**, *7*, e39963. [[CrossRef](#)] [[PubMed](#)]
25. Sabaj, M.H. *Codes for Natural History Collections in Ichthyology and Herpetology (Online Supplement), Version 9.0*; 14 February 2022; American Society of Ichthyologists and Herpetologists: Washington, DC, USA, 2022.

26. Norman, J.R. Coast fishes. Part III. The Antarctic zone. In *Discovery Reports Vol. XVIII.*; Cambridge University Press: Cambridge, UK, 1938; pp. 3–105.
27. Last, P.R.; Weigmann, S.; Yang, L. Changes to the nomenclature of the skates (Chondrichthyes: Rajiformes). *Rays World Suppl. Inf.* **2016**, *CSIRO Special Publication*, 11–34.
28. Franzese, S.; Facal, G.G.; Menoret, A. Tapeworms (Platyhelminthes, Cestoda) from marine chondrichthyans of the Southwestern Atlantic Ocean, and the sub-Antarctic and Antarctic islands: A checklist. *ZooKeys* **2023**, *1163*, 79–119. [[CrossRef](#)]
29. Iwami, T.; Abe, T. Notes on the fishes collected during the 1980–1981 exploratory bottom trawl fishing off the South Shetland Islands. *Mem. Natl. Inst. Polar Res. Spec. Issue* **1982**, *23*, 55–63.
30. Hanchet, S.M.; Stewart, A.L.; McMillan, P.J.; Clark, M.R.; O’Driscoll, R.L.; Stevenson, M.L. Diversity, relative abundance, new locality records, and updated fish fauna of the Ross Sea region. *Antarct. Sci.* **2013**, *25*, 619–636. [[CrossRef](#)]
31. Stehmann, M. Ergebnisse der Forschungsreisen des FFS “Walther Herwig” nach Südamerika. LXIV. *Bathyrāja papilionifera* sp. n. (Pisces, Batoidea, Rajidae), eine weitere neue Rochenart aus dem Südwestatlantik vom nordargentinischen Kontinentabhäng. *Arch. Fischereiwiss.* **1985**, *36*, 195–211.
32. Jones, C.; Damerou, M.; Deitrich, K.; Driscoll, R.; Kock, K.H.; Kuhn, K.; Moore, J.; Morgan, T.; Near, T.; Pennington, J.; et al. Chapter 9. Demersal finfish survey of the South Orkney Islands. In *AMLR 2008/2009 Field Season Report—Objectives, Accomplishments and Tentative Conclusions*, NOAA-TM-NMFS-SWFSC-445; Van Cise, A.M., Ed.; U.S. Department of Commerce, National Oceanic & Atmospheric Administration: La Jolla, CA, USA, 2009; pp. 49–66.
33. Kalisz, H. The Comparison of Two Undescribed Species of Skates, *Bathyrāja* sp. 2 and *Bathyrāja* sp. (c.f. *eatonii*) from the Antarctic Waters of the South Orkney Islands. Bachelor’s Thesis, Wilkes Honors College of Florida Atlantic University, Jupiter, FL, USA, 2013.
34. Stehmann, M.; Bürkel, D.L. Rajidae. In *Fishes of the Southern Ocean*; Gon, O., Heemstra, P.C., Eds.; J.L.B. Smith Institute of Ichthyology: Grahamstown, South Africa, 1990; pp. 86–97.
35. Smith, P.J.; Steinke, D.; Mcveagh, S.M.; Stewart, A.L.; Struthers, C.D.; Roberts, C.D. Molecular analysis of Southern Ocean skates (*Bathyrāja*) reveals a new species of Antarctic skate. *J. Fish Biol.* **2008**, *73*, 1170–1182. [[CrossRef](#)]
36. Stehmann, M.F.W.; Merrett, N.R. First records of advanced embryos and egg capsules of *Bathyrāja* skates from the deep north-eastern Atlantic. *J. Fish Biol.* **2001**, *59*, 338–349. [[CrossRef](#)]
37. Jensen, A.S. *The Selachians of Greenland*; Mindeskrift for Japetus Steenstrup; Bianco Lunos Bogtrykkeri: København, Denmark, 1914.
38. Garrick, J.A.F. Studies on New Zealand Elasmobranchii. Part XIII. A new species of *Raja* from 1300 Fathoms. *Trans. R. Soc. N. Z.* **1961**, *88*, 743–748.
39. Raschi, W.; McEachran, J.D. *Rhinoraja longi*, a new species of skate from the outer Aleutian Islands, with comments on the status of *Rhinoraja* (Chondrichthyes, Rajoidei). *Can. J. Zool.* **1991**, *69*, 1889–1903. [[CrossRef](#)]
40. Herman, J.; Hovestadt-Euler, M.; Hovestadt, D.C.; Stehmann, M. Contributions to the study of the comparative morphology of teeth and other relevant ichthyodorulites in living supraspecific taxa of chondrichthyan fishes. Part B: Batomorphii No. 1b: Order: Rajoidei—Family: Rajidae Genera and Subgenera: *Bathyrāja* (with a deep-water, shallow-water and transitional morphotype), *Psammobatis*, *Raja* (*Amblyrāja*), *Raja* (*Dipturus*), *Raja* (*Leucoraja*), *Raja* (*Raja*), *Raja* (*Rajella*) (with two morphotypes), *Raja* (*Rioraja*), *Raja* (*Rostroraja*), *Raja* (*lintea*) and *Sympterygia*. *Bull. Inst. R. Sci. Nat. Belg.* **1995**, *65*, 237–307.
41. Herman, J.; Hovestadt-Euler, M.; Hovestadt, D.C.; Stehmann, M. Contributions to the study of the comparative morphology of teeth and other relevant ichthyodorulites in living supra-specific taxa of Chondrichthyan fishes. Part B: Batomorphii No. 1c: Order: Rajiformes—Suborder Rajoidei—Family: Rajidae—Genera and Subgenera: *Arhynchobatis*, *Bathyrāja richardsoni*-type, *Cruriraja*, *Irolita*, *Notoraja*, *Pavoraja* (*Insentiraja*), *Pavoraja* (*Pavoraja*), *Pseudoraja*, *Raja* (*Atlantoraja*), *Raja* (*Okamejei*) and *Rhinoraja*. *Bull. Inst. R. Sci. Nat. Belg.* **1996**, *66*, 179–236.
42. Sáez, S.; Lamilla, J. Sexual homodonty in *Bathyrāja griseocauda* (Norman 1937) from the Southern Eastern Pacific (Chile) (Chondrichthyes, Rajidae: Arhynchobatinae). *J. Appl. Ichthyol.* **2004**, *20*, 189–193. [[CrossRef](#)]
43. Scenna, L.B.; García De La Rosa, S.B.; Díaz De Astarloa, J.M. Trophic ecology of the Patagonian skate, *Bathyrāja macloviana*, on the Argentine continental shelf. *ICES J. Mar. Sci.* **2006**, *63*, 867–874. [[CrossRef](#)]
44. Bizikov, V.; Arkhipkin, A.I.; Laptikhovskiy, V.V.; Pompert, J.H.W. *Identification Guide and Biology of the Falkland Skates*; Fisheries Department, Falkland Island Government: Stanley, Falkland Islands, 2004.
45. Stehmann, M. *Bathyrāja tunae* n. sp., a new deep-water skate from the Western Indian Ocean (Chondrichthyes, Rajiformes, Rajidae). *J. Ichthyol.* **2005**, *45*, 23–38.
46. Stehmann, M. *Bathyrāja ishiharai* n. sp., a new deep-water skate from the Eastern Indian Ocean on the Naturalist Plateau off south-western Australia (Elasmobranchii, Rajiformes, Rajidae). *J. Ichthyol.* **2005**, *45*, 39–57.
47. Iglésias, S.P.; Lévy-Hartmann, L. *Bathyrāja leucomelanos*, a new species of softnose skate (Chondrichthyes: Arhynchobatidae) from New Caledonia. *Ichthyol. Res.* **2012**, *59*, 38–48. [[CrossRef](#)]
48. Knuckey, J.D.S.; Ebert, D.A. A taxonomic revision of Northeast Pacific softnose skates (Rajiformes: Arhynchobatidae: *Bathyrāja* Ishiyama). *Zootaxa* **2022**, *5142*, 1–89. [[CrossRef](#)]
49. Deynat, P.P.; Séret, B. Le revêtement cutané des raies (Chondrichthyes, Elasmobranchii, Batoidea). I- Morphologie et arrangement des denticules cutanés. *Ann. Sci. Nat. Zool. Biol. Anim.* **1996**, *17*, 65–83.
50. Deynat, P.P. Le revêtement cutané des raies (Chondrichthyes, Elasmobranchii, Batoidea). II. Morphologie et arrangement des tubercules cutanés. *Ann. Sci. Nat. Zool. Biol. Anim.* **1998**, *19*, 155–172. [[CrossRef](#)]

51. Rangel, B.D.S.; Wosnick, N.; Magdanelo Leandro, R.; Amorim, A.F.D.; Kfoury Junior, J.R.; Rici, R.E.G. Thorns and dermal denticles of skates *Atlantoraja cyclophora* and *A. castelnaui*: Microscopic features and functional implications. *Microsc. Res. Tech.* **2016**, *79*, 1133–1138. [[CrossRef](#)] [[PubMed](#)]
52. McEachran, J.D.; Konstantinou, H. Survey of the variation in alar and malar thorns in skates: Phylogenetic implications (Chondrichthyes: Rajoidei). *J. Morphol.* **1996**, *228*, 165–178. [[CrossRef](#)]
53. Henderson, A.C.; Arkhipkin, A.I.; Chtcherbich, J.N. Distribution, Growth and Reproduction of the White-spotted Skate *Bathyraja albomaculata* (Norman, 1937) Around the Falkland Islands. *J. Northw. Atl. Fish. Sci.* **2004**, *35*, 79–87. [[CrossRef](#)]
54. Gallagher, M.J.; Nolan, C.P.; Jeal, F. The Structure and Growth Processes of Caudal Thorns. *J. Northw. Atl. Fish. Sci.* **2005**, *35*, 125–129. [[CrossRef](#)]
55. Perez, C.R.; Cailliet, G.M.; Ebert, D.A. Age and growth of the sandpaper skate, *Bathyraja kincaidii*, using vertebral centra, with an investigation of caudal thorns. *J. Mar. Biol. Ass.* **2011**, *91*, 1149–1156. [[CrossRef](#)]
56. Deynat, P. Applications de l'étude du Revêtement Cutané des Chondrichthyens à la Systématique Phylogénétique des pristiformes et des Rajiformes *sensu* Compagno, 1973 (Elasmobranchii, Batoidea). Ph.D. Thesis, l'Université Paris, Paris, France, 1996.
57. Nowara, G.B.; Burch, P.; Gasco, N.; Welsford, D.C.; Lamb, T.D.; Chazeau, C.; Duhamel, G.; Pruvost, P.; Wotherspoon, S.; Candy, S.G. Distribution and abundance of skates (*Bathyraja* spp.) on the Kerguelen Plateau through the lens of the toothfish fisheries. *Fish. Res.* **2017**, *186*, 65–81. [[CrossRef](#)]
58. Finucci, B.; Charles, R. *Bathyraja arctowskii*. In *The IUCN Red List of Threatened Species: E.T211718188A211718843*; IUCN Global Species Programme Red List Unit: Cambridge, UK, 2022.
59. Commission for the Conservation of Antarctic Marine Living Resources (CCAMLR). *Conservation Measure 22-08 (2009) Prohibition on Fishing for Dissostichus spp. in Depths Shallower than 550 m in Exploratory Fisheries 2009*; Commission for the Conservation of Antarctic Marine Living Resources: Hobart, Australia, 2009.
60. Commission for the Conservation of Antarctic Marine Living Resources (CCAMLR). *Conservation Measure 91-05 (2016) Ross Sea region Marine Protected Area 2016*; Commission for the Conservation of Antarctic Marine Living Resources: Hobart, Australia, 2016.

Disclaimer/Publisher's Note: The statements, opinions and data contained in all publications are solely those of the individual author(s) and contributor(s) and not of MDPI and/or the editor(s). MDPI and/or the editor(s) disclaim responsibility for any injury to people or property resulting from any ideas, methods, instructions or products referred to in the content.